Meson Spectroscopy: Glueballs, Hybrids and $Q\bar{Q}$ Mesons

Eberhard Klempt *

Institut für Strahlen– und Kernphysik
der Universität Bonn
D-53115 BONN

Abstract

Lattice gauge calculations predict the existence of glueballs. In particular a scalar glueball is firmly expected at a mass of about 1730 MeV. This prediction has led to an intense study of scalar isoscalar interactions and to the discovery of new meson resonances. The number of scalar states observed seems to exceed the number of states which can be accommodated in the quark model even when two states, the $a_0(980)$ and $f_0(980)$, are interpreted as $K\bar{K}$ bound states and are removed from the list. However, none of these states has a decay pattern which is consistent with that of a pure glueball. A reasonable interpretation of the number of states and of their decay pattern is found only when mixing of scalar $q\bar{q}$ states with the scalar glueball is taken into account.

In this paper we scrutinize the evidence for these states and their production characteristics. The $f_0(1370)$ - a cornerstone of all $q\bar{q}$-glueball mixing scenarios - is shown to be likely of non-$q\bar{q}$ nature. The remaining scalar states then do fit into a nonet classification. If this interpretation should be correct there would be no room for resonant scalar gluon-gluon interactions, no room for the scalar glueball.

We also discuss the status of mesons with exotic quantum numbers, of mesons which cannot possibly have $q\bar{q}$ structure, and argue that these are, most likely, four-quark states and not excitations of the gluon string providing the binding between quark and antiquark.

* *Electronic mail address: klempt@iskp.uni-bonn.de*

1 Introduction: why hadron spectroscopy ?

SU(3) symmetry considerations had shown to be extremely useful in classifying mesons and baryons [1] as composed of quarks and antiquark or of 3 quarks, respectively. Deep inelastic scattering had provided early insight into the physics of partons [2]. At that time, the concept of particles carrying charges of one or two thirds of the electron charge was, however, too far away from every-days experience, and the reality of quarks was often not accepted. The breakthrough of the quark model in the general perception of physicist was the discovery of the J/ψ family of meson resonances [3, 4] and their interpretation of $\bar{c}c$ states [5]. Attempts to find conventional explanations for the new narrow states as $\omega\omega$ ccompounds or $\bar{\text{p}}$p resonances [6, 7] failed, and the quark model became the frame of further progress in the field. A new theory of strong interactions, Quantum Chromo Dynamics or QCD, emerged [8, 9] which assigned to quarks a new triple-valued charge called color. The fact that free quarks were never observed was understood by the hypothesis that color is confined [10], even though their mutual interactions were supposed to be weak at large momentum transfers or at small distances [11]. Particles which we observe in nature must be color-neutral. Color-neutral objects can be formed by combining a colored quark and an antiquark with anticolour to a meson or by combining 3 quarks with 3 different colors to a baryon.

According to the Standard Model we have 3 generations of quarks and leptons which are shown in Fig. 1. The unified theory of electromagnetic and weak interactions, Quantum Flavor Dynamics, acts within the plane of Fig. 1; strong interactions are restricted to the exchange of color via gluons and act in the third direction. This latter interaction is of relevance for the further discussion. It is a renormalisable gauge field theory constructed in line with QED. Unfortunately, this beautiful theory is of limited use in hadron spectroscopy; calculations can be carried out only at large momentum transfer, in the realm of perturbative QCD. Only there, observables can be expressed in a power series in fine-structure constant α_s of strong interaction.

Another limit in which QCD can be solved is at very small energies. The light quarks u, d are nearly massless, also the strange quark mass is small. In the limit of vanishing masses there is a new symmetry, chiral symmetry: massless particles cannot flip spin. This symmetry is spontaneously broken and massless pseudoscalar bosons, Goldstone bosons must exist [12]. Finite quark masses lead to a breaking of chiral symmetry in the Lagrangian, the Goldstone bosons acquire mass and can be identified with the pseudoscalar mesons. At small energies, the breaking of chiral symmetry can be treated perturbatively, and we have access to QCD.

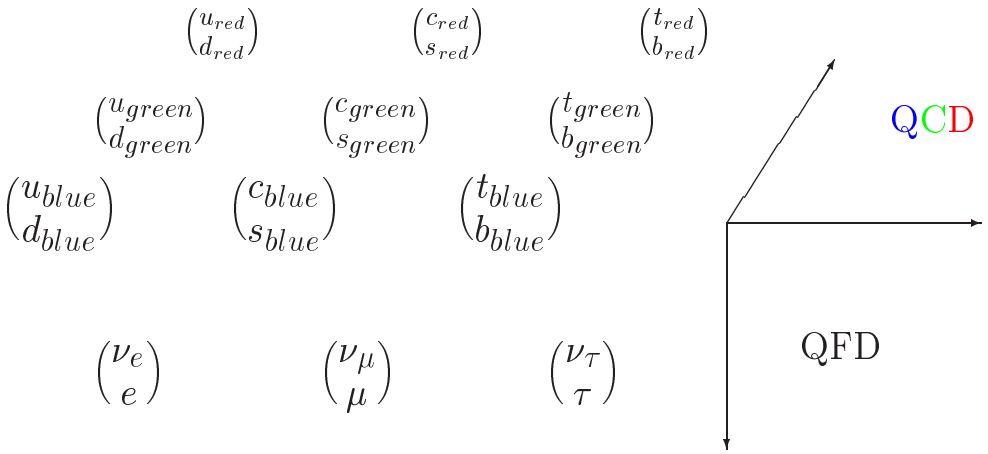

Figure 1: The Standard Model

The situation is worse at medium energies, in the resonance region. This is the domain of Strong QCD. The interaction becomes very strong and an expansion in the strong-interaction fine-structure constant α_s is meaningless. The different fields in which QCD acts are summarized in Fig. 2.

To understand what QCD tells us about the range of Q^2 from 0.1 to 4 GeV^2, 'QCD-inspired models' have been developed. These models may guide us in our attempt to understand the effective degrees of freedom in meson and baryon spectroscopy and the effective interaction between them. E.g. we may ask, if we can understand spectroscopy by introducing 'constituent' quarks with an effective mass. If this should be the case, we have to ask what is the residual strong interaction when a part of the interaction has been taken into account by increasing the current quark mass to an effective one.

A large number of such QCD-inspired models have been proposed, like bag models [13], quark models with various quark-quark potentials [14], the Nambu Jona-Lasinio model [15], the flux tube model [16], models based on instanton interactions [17], QCD sum rules [18], or lattice QCD. The latter model claims best reliability; QCD is simulated on a lattice, the lattice points are connected by links representing the gluon fields which adjust itself to provide a minimum energy in a given configuration. Lattice gauge calculations are believed to reproduce the continuum theory for a sufficiently large number of lattice points at smaller and smaller distances.

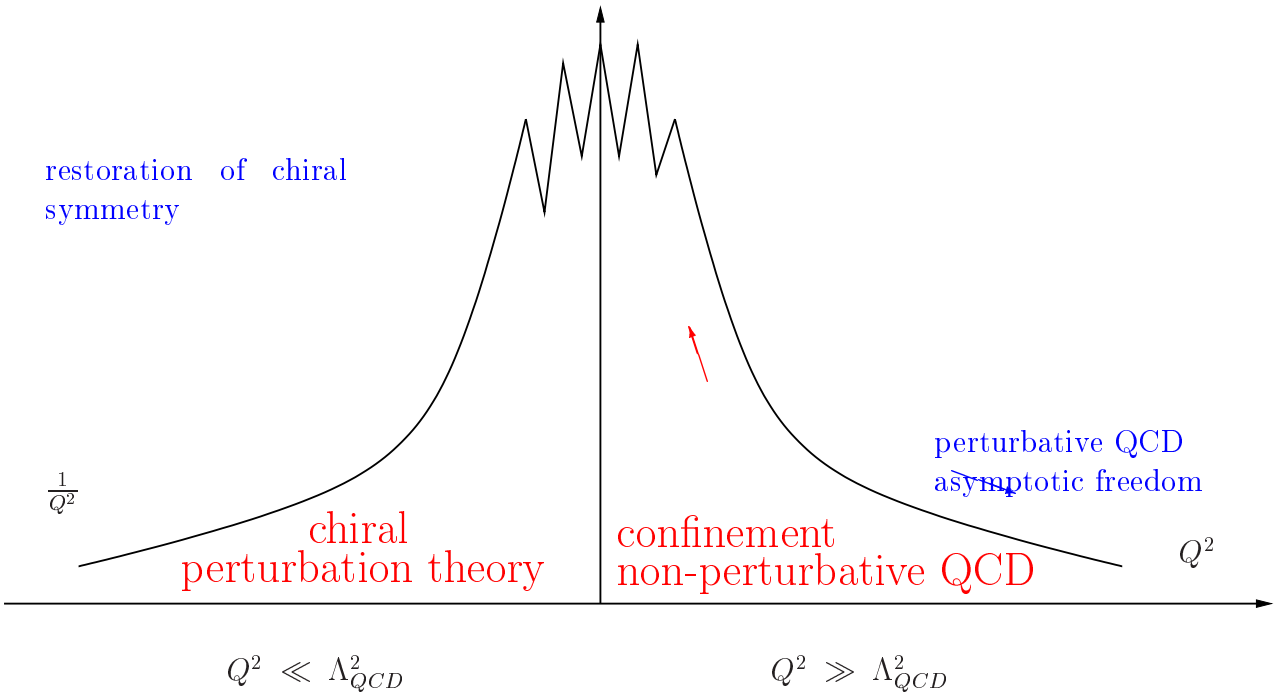

Figure 2: QCD observables as a function of Q^2

Indeed, QCD on a lattice provides a good estimate for the potential between a bottom quark and its antiquark. The potential is shown in Fig. 3. It is well described by a sum a of Coulomb-like term plus a linear (confining) potential:

$$V(r) = V_0 + \frac{4}{3}\frac{\alpha_s}{r} + cr \tag{1}$$

At small distances the potential is dominated by the Coulomb-like part, with a coupling constant α_s. The coupling constant is not really a constant; its value is about 0.12 at the Z^0 mass and increases at low energies. At large distances, in the confinement region, the potential energy increases linearly; in the lattice calculation shown in Fig. 3 up to 1.6 fm. The measured masses of $b\bar{b}$ states are well reproduced by the lattice calculations, see Fig. 4.

We may get access to very large quark-antiquark separations by considering high-spin states. Fig. 5 shows that the spin of $q\bar{q}$ resonances are linearly related to their squared masses. We can understand this relation assuming that the gluon flux between the two quarks is concentrated in a rotating flux tube or a rotating string with a homogeneous mass density. The velocity at the ends may be the velocity of light. Then the total mass of the string is

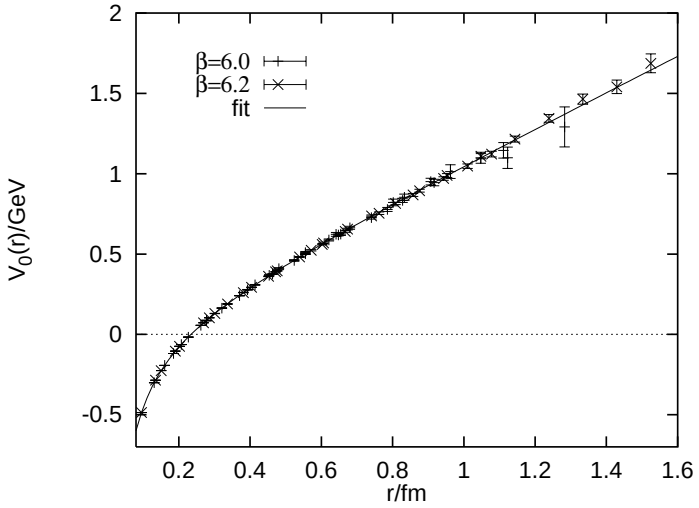

Figure 3: $b\bar{b}$ potential from lattice calculations; (from [19]).

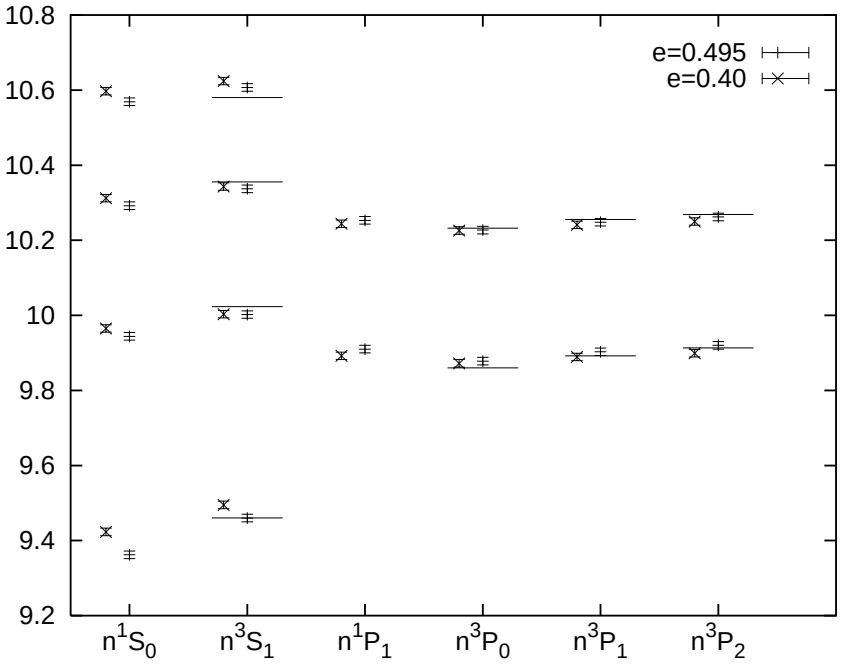

Figure 4: Comparison of Y states from lattice calculations with data (-); (from [20]).

given by

$$Mc^2 = 2\int_0^{r_0} \frac{kdr}{\sqrt{1 - v^2/c^2}} = kr_0\pi$$

and the angular momentum by

$$J = \frac{2}{\hbar c^2}\int_0^{r_0} \frac{krvdr}{\sqrt{1 - v^2/c^2}} = \frac{kr_0^2\pi}{2\hbar c}$$

$$\text{Hence} \qquad J = \frac{1}{2\pi k\hbar c}E^2 + \text{constant}$$

From the slope in Fig. 5 we find $k = 0.2\,\text{GeV}^2$ and radii of

$$r_0(\rho) = 1.2\text{fm} \qquad r_0(a_6) = 4\text{fm}$$

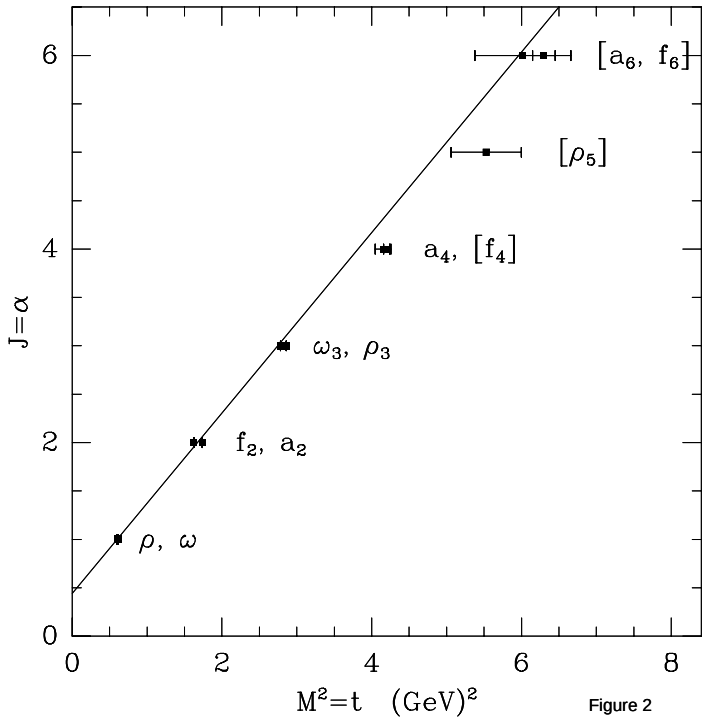

Figure 5: Spin of meson resonances versus M^2. In the Regge theory, non-integer spins α are allowed in exchange processes. Particles have integer spins.

The $a_6^+(2450)$ is a meson with a mass of 2450 MeV in which a u quark and a $\bar{d}$ quark are bound by the confining forces; both quark spins are parallel with the orbital angular momentum $l = 5\hbar$. Quark and antiquark are separated by 8 fm !

The type of potential given in (1) was independently suggested to fit the mass spectrum of the J/ψ and Y families of states. This phenomenological

approach yielded a very similar potential; hence we may conclude (and there are many other examples) that QCD can be simulated on a lattice.

So far, so good. But QCD on the lattice predicts also one new peculiar type of hadronic matter which does not comprise constituent quarks, it predicts glueballs. The search for glueballs has stimulated the field and has led to extensive searches for these states. Many glueball candidates have been suggested in the past; also at present there are reasons to believe that a glueball has been traced in the spectrum of scalar mesons. Personally, I do not share this view. Hence I will discuss the evidence which exists for the scalar glueball, and why I think that data tell us that glueballs may not exist at all.

Apart from glueballs, also bound states of $q\bar{q}$+gluon are expected to exist. The color 3 of a quark and the $\bar{3}$ of an antiquark may form a color singlet: that is then a observable state. But colour 3 and $\bar{3}$ can also couple to 8 which can be colour-neutralized by one gluon (which is always colour 8). These states are called hybrids. You may also think of haybrids as a vibrating color flux tube, as an excitation of the gluon field.

The low-mass glueballs have quantum numbers like other mesons; hence they would show up in the spectrum of mesons as additional states. Hybrids may have quantum numbers which are not accessible to normal $q\bar{q}$ mesons. Therefore it seems appropriate to continue with a short review of the properties of $q\bar{q}$ mesons.

2 The quark model

2.1 Mesons and their quantum numbers

Quarks have spin 1/2 and baryon number 1/3; antiquarks have spin 1/2 and baryon number -1/3. Quark and antiquark combine to B=0 and to spin $S = 1$ or $S = 0$ thus forming conventional mesons. The total spin $\vec{S}$ and the orbital angular momentum $\vec{L}$ between quark and antiquark couple to the total angular momentum $\vec{J}$: $\vec{J} = \vec{L} + \vec{S}$. forming conventional mesons. As $q\bar{q}$ objects they may have the following properties:

2.1.1 Parity $P = (-1)^{L+1}$

The parity of a meson is due to the orbital angular momentum between quark and antiquark $P = (-1)^L$ multiplied with their intrinsic parities $P_q \cdot P_{\bar{q}} =$ -1.

2.1.2 C-Parity $C = (-1)^{L+S}$

The total wave function of a meson is antisymmetric w.r.t. the exchange of quark and antiquark. The symmetry of the wave function is given by the product of symmetries of the spatial and spin wave function, and by the C-parity:

Spins:	$(-1)^{S+1}$	
Space:	$(-1)^{L}$	The product is -1, hence
Charge:	C	

$$C = (-1)^{S+L+1} = -1 \quad \text{and} \quad C = (-1)^{S+L}$$

2.1.3 Isospin

Proton and neutron form an isospin doublet and so do the *up* and the *down* quark. We may construct states of 2 or 3 quarks; the isospin of the system is determined by adding the quark isospins using Clebsch-Gordan coefficients. We could also define $\bar{u}$ and $\bar{d}$ as isospin doublet in a isospin space of antiparticles and invent a new table of Clebsch-Gordan coefficients. Or we can define iso-doublets in a way that the doublets of antiparticle transform under isospin rotations like those of particle doublets. These are, e.g.:

$$\begin{pmatrix} p \\ n \end{pmatrix} \quad \begin{pmatrix} u \\ d \end{pmatrix} \quad \begin{pmatrix} \mathrm{K}^{+} \\ \mathrm{K}^{0} \end{pmatrix} \quad \begin{pmatrix} \mathrm{K}^{*+} \\ \mathrm{K}^{*0} \end{pmatrix}$$

$$\begin{pmatrix} -\bar{n} \\ \bar{p} \end{pmatrix} \quad \begin{pmatrix} -\bar{d} \\ \bar{u} \end{pmatrix} \quad \begin{pmatrix} -\bar{\mathrm{K}}^{0} \\ \mathrm{K}^{-} \end{pmatrix} \quad \begin{pmatrix} \bar{\mathrm{K}}^{*0} \\ -\mathrm{K}^{*-} \end{pmatrix}$$

We now can contruct $q\bar{q}$ mesons like pions or η's.

$$\begin{array}{lcccl}
|I=1, I_3=1> & = & -|u\bar{d}> & = & -|\pi^{+}> \\
|I=1, I_3=0> & = & \frac{1}{\sqrt{2}}(|u\bar{u}> - |d\bar{d}>) & = & |\pi^{0}> \\
|I=1, I_3=-1> & = & |d\bar{u}> & = & |\pi^{-}>
\end{array}$$

$$|I=0, I_3=0> \quad = \quad \frac{1}{\sqrt{2}}(|u\bar{u}> + |d\bar{d}>) \quad = \quad |''\eta''>$$

The three states -$|\pi^{+}>$, $|\pi^{0}>$ and $|\pi^{-}>$ form an iso-triplet, η and η' both form isosinglets.

2.1.4 G-parity $P = (-1)^{L+1+I}$

The C-parity has a defined eigenvalue only for particles which are their own antiparticles. The action of C-parity on other states leads to their antiparticles. We define

$$\mathrm{C}\ |\pi^0> \ = \ +|\pi^0>; \quad \mathrm{C}\ |\pi^+> \ = \ |\pi^->; \quad \mathrm{C}\ |\pi^-> \ = \ |\pi^+>$$

It is useful to introduce also a G-parity as C-parity followed by a rotation in isospin space by 90° about the y-axis. The rotation by 180° in isospin space around y-axis are given by

$$\mathbf{e^{i\pi I_y}}$$

We define: $\mathbf{G = C \cdot e^{i\pi I_y}}$ and introduce *Cartesian states*:

$$|\pi^\pm> \ = \frac{1}{\sqrt{2}} \mid \pi^x \pm \ i\pi^y > \qquad \text{Then :}$$

$$G|\pi^\pm> \ = \ C\frac{1}{\sqrt{2}} e^{i\pi I_y} \mid \pi^x \pm \ i\pi^y >$$

$$C\frac{1}{\sqrt{2}} \mid -\pi^x \pm \ i\pi^y >= (-1)C \mid \pi^\mp >= - \mid \pi^\pm >$$

$$G|\pi^0> \ = \ Ce^{i\pi I_y}|\pi^0> = -C|\pi^0> = -|\pi^0>$$

Thus we have: $G|\pi> = -|\pi>$

G-parity is conserved in strong interactions. For mesons decaying into n_π pions we have the relation

$$G = (-1)^I \cdot C = (-1)^{L+S+I} = (-1)^{n_\pi}$$

2.2 Meson nonets

Mesons are characterized by their quantum numbers J^{PC} and by their flavor content. In SU(3), i.e. in the light-quark domain, a set of quantum numbers J^{PC} leads to a nonet of states. Based on SU(3) symmetry, we expect an octet and a singlet. However, the s quark is heavier than the u and d quark. The three pairs $u\bar{u}$, $d\bar{d}$ and $s\bar{s}$ can therefore form mesons which are approximately SU(3) eigenstates or - approximately - mesons composed of $u\bar{u}$ and $d\bar{d}$ or $s\bar{s}$ pairs.

2.2.1 The pseudoscalar mesons

The pseudoscalar quantum numbers are $J^{PC} = 0^{-+}$. From atomic physics we take the spectroscopic notation $n^{2s+1}L_J = 1^1S_0$. From the 3 quarks u, d, s and their antiquarks the following SU(3) eigenstates can be constructed:

$$K^0 = d\bar{s} \qquad K^+ = u\bar{s}$$

$$\pi^- = d\bar{u} \qquad \pi^0 = \frac{1}{\sqrt{2}}(u\bar{u} - d\bar{d}) \qquad \pi^+ = u\bar{d}$$

$$K^- = s\bar{u} \qquad K^0 = s\bar{d}$$

$$\eta_8 = \sqrt{\frac{1}{6}}(u\bar{u} + d\bar{d} - 2s\bar{s}) \qquad \eta_1 = \sqrt{\frac{1}{3}}(u\bar{u} + d\bar{d} + s\bar{s})$$

The 9 states are orthogonal; one of them, the η_1, is invariant under rotations in SU(3). The nonet structure is seen in the well-known nonet representation:

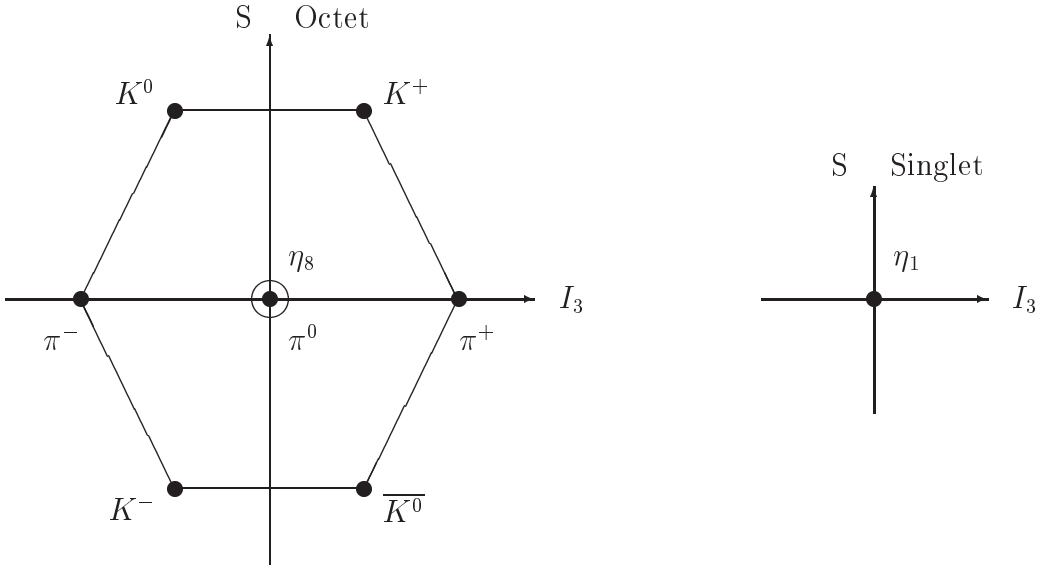

The octet state and the singlet state are the SU(3) eigenstates. They have the same quantum numbers and can mix. The mixing angle is called pseudoscalar mixing angle Θ_{PS}. The physical states are given by

$$|\eta> = \cos\Theta_{PS}|\eta_8> - \sin\Theta_{PS}|\eta_1>$$

$$|\eta'> = \sin\Theta_{PS}|\eta_8> + \cos\Theta_{PS}|\eta_1>$$

We can write down the flavor wave function for a few angles:

$$
\begin{array}{lcll}
\Theta_{PS} = & 0^\circ & |\eta> & = & \frac{1}{\sqrt{6}}\left(u\bar{u}+d\bar{d}-2s\bar{s}\right) \\
 & & |\eta'> & = & \frac{1}{\sqrt{3}}\left(u\bar{u}+d\bar{d}+s\bar{s}\right) \\
\Theta_{PS} = & -11.1^\circ & |\eta> & = & \frac{1}{\sqrt{2}}\left(\frac{1}{\sqrt{2}}(u\bar{u}+d\bar{d})-s\bar{s}\right) \\
 & & |\eta'> & = & \frac{1}{\sqrt{2}}\left(\frac{1}{\sqrt{2}}(u\bar{u}+d\bar{d})+s\bar{s}\right) \\
\Theta_{PS} = & -19.3^\circ & |\eta> & = & \frac{1}{\sqrt{3}}\left(u\bar{u}+d\bar{d}-s\bar{s}\right) \\
 & & |\eta'> & = & \frac{1}{\sqrt{6}}\left(u\bar{u}+d\bar{d}+2s\bar{s}\right) \\
\Theta_{PS} = & 35.3^\circ & |\eta> & = & s\bar{s} \\
 & & |\eta'> & = & \frac{1}{\sqrt{2}}\left(u\bar{u}+d\bar{d}\right)
\end{array}
$$

The large mixing between the $\sqrt{\frac{1}{2}}(u\bar{u}+d\bar{d})$ (which we abbreviate as $n\bar{n}$) and the $s\bar{s}$ component in the η and η' wave functions has led to speculations that the η and in particular the η' may contain a large fraction of glue, that they are *gluish*. This requires an extension of the mixing scheme by introduction of a non-$q\bar{q}$ or *inert* component, with a third state of unknown mass which is dominantly a glueball.

$$
\begin{array}{lccc}
|\eta> = & X_\eta \cdot \frac{1}{\sqrt{2}}\left(u\bar{u}+d\bar{d}\right) + & Y_\eta \cdot (s\bar{s}) + & Z_\eta \cdot (\text{glue}) \\
|\eta'> = & X_{\eta'} \cdot \frac{1}{\sqrt{2}}\left(u\bar{u}+d\bar{d}\right) + & Y_{\eta'} \cdot (s\bar{s}) + & Z_{\eta'} \cdot (\text{glue}) \\
 & \text{light quark} & \text{strange quark} & \text{inert} \\
 & & & Z_\eta = Z_{\eta'} \sim 0
\end{array}
$$

Indeed, a first systematic survey of J/ψ decays into vector and pseudoscalar mesons suggested that the η' may contain a large glueball fraction ($\sim 35\%$) [21]. At that time, the $\iota(1440)$ or $\eta(1440)$ was believed to have a large glueball fraction and mixing of η, η', and $\eta(1440)$ was held responsible for the gluish nature of the η'. Yet later more precise data excluded this possibility [22, 23]. Nevertheless, this question remained a controversial topic since then. In a very recent article it was shown that there is no need to introduce glue into the η' wave function [24].

At present there is no convincing evidence for a glueball content in the η' wave function; nevertheless the η' is still suspect of being produced preferentially in glue-rich processes or in glueball decays.

2.2.2 Vector and tensor mesons

On the next page we show - without further comments - the nonet of vector and tensor mesons with $J^{PC} = 1^{--}$ and with 2^{++}, respectively, or of the 1^3S_1

L	S	J	n	I=1	I=1/2	I=0	I=0	J^{PC}	$n^{2s+1}L_J$
0	0	0	1	π	K	η'	η	0^{-+}	1^1S_0
0	1	1	1	ρ	K^*	Φ	ω	1^{--}	1^3S_1
1	0	1	1	$b_1(1235)$	K_{1B}	$h_1(1380)$	$h_1(1170)$	1^{+-}	1^1P_1
1	1	0	1	$a_0(????)$	$K_0^*(1430)$	$f_0(????)$	$f_0(????)$	0^{++}	1^3P_0
1	1	1	1	$a_1(1260)$	K_{1A}	$f_1(1510)$	$f_1(1285)$	1^{++}	1^3P_1
1	1	2	1	$a_2(1320)$	$K_2^*(1430)$	$f_2(1525)$	$f_2(1270)$	2^{++}	1^3P_2
2	0	2	1	$\pi_2(1670)$	$K_2(1770)$	$\eta_2(1645)$	$\eta_2(1870)$	2^{-+}	1^1D_2
2	1	1	1	$\rho(1700)$	$K^*(1680)$	$\omega(1650)$	$\Phi(????)$	1^{--}	1^3D_1
2	1	2	1	$\rho_2(????)$	$K_2(1820)$	$\omega_2(????)$	$\Phi_2(????)$	2^{--}	1^3D_2
2	1	3	1	$\rho_3(1690)$	$K_3^*(1780)$	$\omega_3(1670)$	$\Phi_3(1850)$	3^{--}	1^3D_3
0	0	0	2	$\pi(1370)$	$K_0(1460)$	$\eta(????)$	$\eta(1440)$	0^{-+}	2^1S_0
0	1	1	2	$\rho(1450)$	$K^*(1450)$	$\Phi(1680)$	$\omega(1420)$	1^{--}	2^3S_1

Table 1: The light mesons. The two mesons K_{1A} and K_{1B} mix to form the observed resonances $K_1(1280)$ and $K_1(1400)$. The two η_2 states are from [28]. In some cases, mesons still need to be identified. The scalar mesons resist an unambiguous classification.

and 1^3P_2 states. Both nonets have a nearly *ideal mixing angle* $\Theta_{ideal} = 35.3°$ for which one meson is a purely $s\bar{s}$ state. Note that the mass difference between the $s\bar{s}$ and the $u\bar{u} + d\bar{d}$ state is about 250 MeV.

2.2.3 Other meson nonets

A meson nonet is fully described by just 4 names. The pseudoscalar nonet contains 3 pions, four kaon, the η' and the η. In Table 1 some meson nonets are collected. The $f_1(1510)$ is chosen as $s\bar{s}$state instead of the $f_1(1420)$ as only the former has mass and decay modes compatible with values expected from SU(3) arguments [25]. The $\eta(1295)$ is mostly considered to be the radial excitation of the η ground state. This assignment is challenged by its non-observation in radiative J/ψ decays, in $\bar{p}p$ annihilation [26] and in 2-photon collisions [27] while the $\eta(1440)$ is observed in all three reactions.

The vector mesons $J^{PC} = 1^{--}$

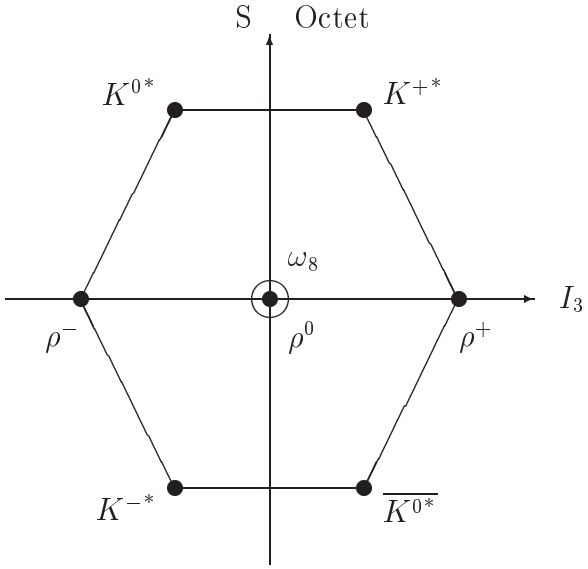

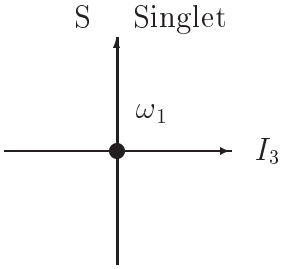

The tensor mesons $J^{PC} = 2^{++}$

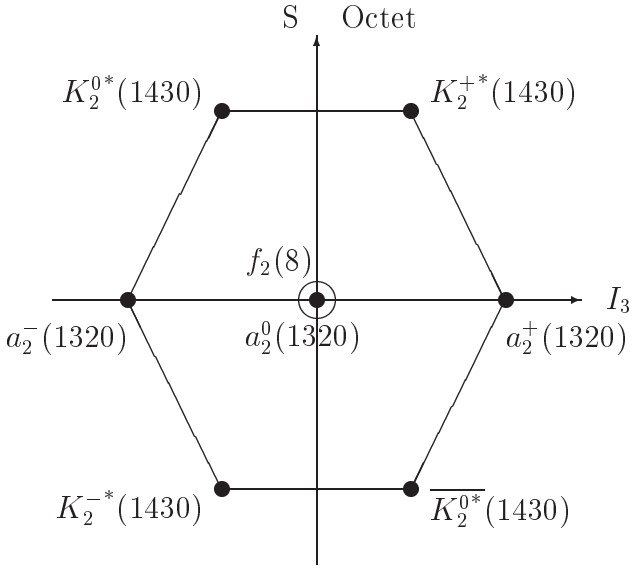

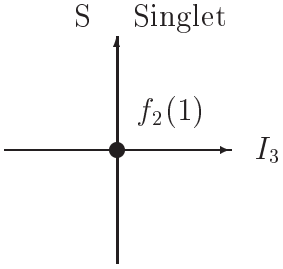

$\Theta_{V,T} = 35.3^\circ$	$\|\omega>$	$=$	$\frac{1}{\sqrt{2}}\left(u\bar{u} + d\bar{d}\right)$	$\sim$	$f_2(1270)$
	$\|\Phi>$	$\sim$	$s\bar{s}$	$=$	$f_2(1525)$

2.2.4 The Gell-Mann-Okubo mass formula

You can derive a relation between the masses within a meson nonet by ascribing to mesons of one nonet a common mass M_0 plus the (constituent) masses of the quark and antiquark it is composed of. The pion mass is given by

$$M_\pi = M_0 + 2M_q$$

where M_q is the mass of the up or down quark, and the Kaon mass by

$$M_K = M_0 + M_q + M_s$$

with M_s as strange quark mass. The η contains masses from both the singlet and octet component which we weight according to their fractions:

$$M_\eta = M_8 \cos^2\Theta + M_1 \sin^2\Theta$$

$$M_{\eta'} = M_8 \sin^2\Theta + M_1 \cos^2\Theta$$

Similarly we determine the singlet and octet masses from the flavor decomposition of their wave functions.

$$M_1 = M_0 + 4/3M_q + 2/3M_s$$

$$M_8 = M_0 + 2/3M_q + 4/3M_s$$

Thus we arrive at the linear mass formula:

$$\cos^2\Theta = \frac{3M_\eta + M_\pi - 4M_K}{4M_K - 3M_{\eta'} - M_\pi}$$

Often, the linear GMO mass formula is replaced by the quadratic GMO formula which is given as above but with M^2 values instead of masses. It reads

$$\cos^2\Theta = \frac{3M_\eta^2 + M_\pi^2 - 4M_K^2}{4M_K^2 - 3M_{\eta'}^2 - M_\pi^2}$$

Nonet members	Θ_{linear}	Θ_{quad}
π, K, η', η	$-23°$	$-10°$
$\rho, K^*, \Phi\ , \omega$	$36°$	$39°$
$a_2(1320), K_2^*(1430), f_2(1525), f_2(1270)$	$26°$	$29°$
$\rho_3(1690), K_3^*(1780), \Phi_3(1850)\ , \omega_3(1670)$	$29°$	$28°$

2.2.5 Meson decays

The decays of mesons belonging to a given nonet are related by SU(3) symmetry. The coefficients governing these relations are called SU(3) isoscalar factors and listed by the Particle Data Group [29]. We show here two simple examples.

A glueball is, by definition, a flavor singlet. It may decay into two octet mesons. Hence we have the decay $1 \to\ 8 \times\ 8$. In the listings we find

$$(\Lambda) \to\ (N\bar{K}\ \ \Sigma\pi\ \ \Lambda\eta\ \ \Xi K) = \frac{1}{\sqrt{8}}(2\ \ 3\ \ -1\ \ -2)^{1/2}$$

The particles stand for their SU(3) assignment, the Λ can be octet or singlet. The $^{1/2}$ is understood for every coefficient. Translated into decays of a flavor singlet meson into two pseudoscalar mesons it reads

$$(\text{glueball}) \to\ (K\bar{K}\ \ \pi\pi\ \ \eta_8\eta_8\ \ \bar{K}K) = \frac{1}{\sqrt{8}}(2\ \ 3\ \ -1\ \ -2)^{1/2}$$

Hence glueballs have squared couplings to $\mathrm{K\bar{K}}$, $\pi\pi$, $\eta_8\eta_8$ of $4:3:1$. The decay into two isosinglet mesons $\eta_1\eta_1$ has an independent coupling and is not restricted by these SU(3) relations. The decay into $\eta_1\eta_8$ is forbidden: a singlet cannot decay into a singlet and an octet meson. This selection rule holds even for any pseudoscalar mixing angle: the two mesons η and η' have orthogonal SU(3) flavor states and a flavor singlet cannot dissociate into two states which are orthogonal.

As second example we choose decays of vector mesons into two pseudoscalar mesons. We compare the two decays $\mathrm{K^*{\to}K}\pi$ and $\rho{\to}\pi\pi$. These are decays of octet particles into two octet particles, $8 \to\ 8 \times 8$. Two octets can couple to an octet with symmetry or antisymmetry w.r.t. their exchange. The two pions in ρ decay must be antisymmetric, hence we have to use the isoscalar factors for $8_2 \to\ 8 \times 8$.

$$(K^*) \to\ (K\pi\ \ K\eta\ \ \pi K\ \ \eta K) = \frac{1}{\sqrt{12}}(3\ \ 3\ \ 3\ \ -3)^{1/2}$$

$$(\rho) \to\ (K\bar{K}\ \ \pi\pi\ \ \eta\pi\ \ \pi\eta\ \ \bar{K}K) = \frac{1}{\sqrt{12}}(2\ \ 8\ \ 0\ \ 0\ \ -2)^{1/2}$$

Hence we derive $\mathrm{K^*{\to}K}\pi{+}\pi\mathrm{K} \propto\ 6$, $\rho{\to}\pi\pi \propto\ 8$, or

$$\frac{\Gamma_{K^*\to K\pi+\pi K}}{\Gamma_{\rho\to\pi\pi}} = \frac{6}{8}\left(\frac{0.291}{0.358}\right)^3 = 0.40$$

The latter factor is the ratio of the decay momenta q to the 3rd power. The transition probability is proportional to q; for low momenta, the centrifugal barrier scales with q^{2l} where l is the angular momentum.

From data we know that the width ratio is 0.34. So the relations are o.k. at the level of $\sim 20\%$. This is a typical level of SU(3) breaking effects. We have neglected many things: mesons have a size; the ρ and K^* sizes are different; the angular barrier factor should include Blatt-Weisskopf corrections. An application of SU(3) to vector and tensor mesons can be found in [30].

2.2.6 Scalar mesons

Of particular interest is the spectrum of scalar mesons since the lowest-mass glueball is expected to have quantum numbers $J^{PC} = 0^{++}$ or 1^3P_0 (see Fig. 6). Unfortunately, the information on scalar mesons is not unique. A few years ago, only little was known about scalar mesons. The experimental situation has improved in the meanwhile but the discussion is still controversial. Below you find the ground state nonet of scalar mesons as most physicists in the field would agree upon. Clearly, the situation is unsatisfactory. There is a number of candidates to fill in the question marks but there is no general agreement which meson should go where.

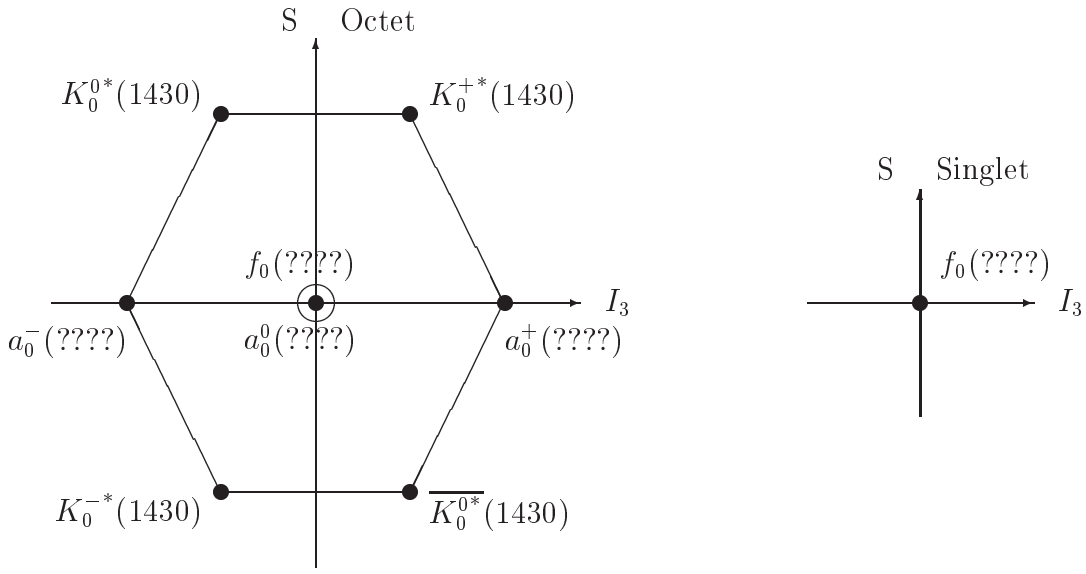

2.3 Beyond the quark model

Mesons which are composed of a constituent quark and antiquark are referred to as conventional mesons. In addition, other forms of hadronic matter are supposed to exist. These are glueballs, excitations of the QCD vacuum or hadrons without any constituent quark, hybrids, hadrons in which the gluonic string mediating the color flux between quark and antiquark is excited, or multiquark states with 2 or 3 $q\bar{q}$ pairs as constituent particles. If two (three) $q\bar{q}$ pairs are clustered into two separate mesons (nucleons), we speak of mesonic molecules or of quasi-nuclear states.

In the next sections of this manuscript I will concentrate on new information on scalar mesons and will attempt my own interpretation. It has the disadvantage that very few physicists working in the field will agree to this view, it has the advantage that it is what I believe to be close to the 'truth'. Physicists who disagree with the view presented here may check their favored interpretation against the experimental findings and the consequences drawn here.

An excellent and unbiased modern review of meson spectroscopy can be found in [31]. There are many open questions at present concerning glueballs and hybrids; these are discussed in detail in this report.

3 Glueballs and their ground state

Glueballs and hybrids reflect new degrees of freedom brought into hadron spectroscopy by QCD and are therefore of prime interest. Indeed, the main motivation of current experiments on meson spectroscopy is the quest to search for glueballs and hybrids, to establish their non-$q\bar{q}$ character and to determine their properties: masses, total and partial widths, and their mixing with ordinary $q\bar{q}$ states having the same quantum numbers. There are indeed strong candidates, both for glueballs and for hybrids. The number of scalar states with $I^G(J^{PC}) = 0^+(0^{++})$ seems to be too large to be accommodated within the quark model. On the other hand, none of the states has decay properties as expected for a pure glueball. Mixing scenarios have hence been proposed in which the pattern of observed states is understood as quarkonia mixing with a primordial glueball intruding into the $q\bar{q}$ world. The discussion of the scalar mesons is the content of this section.

3.1 Where to find glueballs and how

3.1.1 Glueballs and their masses

The most trusted predictions for the glueball mass spectrum are based on lattice gauge calculations. They have become increasingly precise with the advent of high-speed computers and new and efficient codes. Fig. 6 shows a recent calculation of the glueball mass spectrum. The ground state is

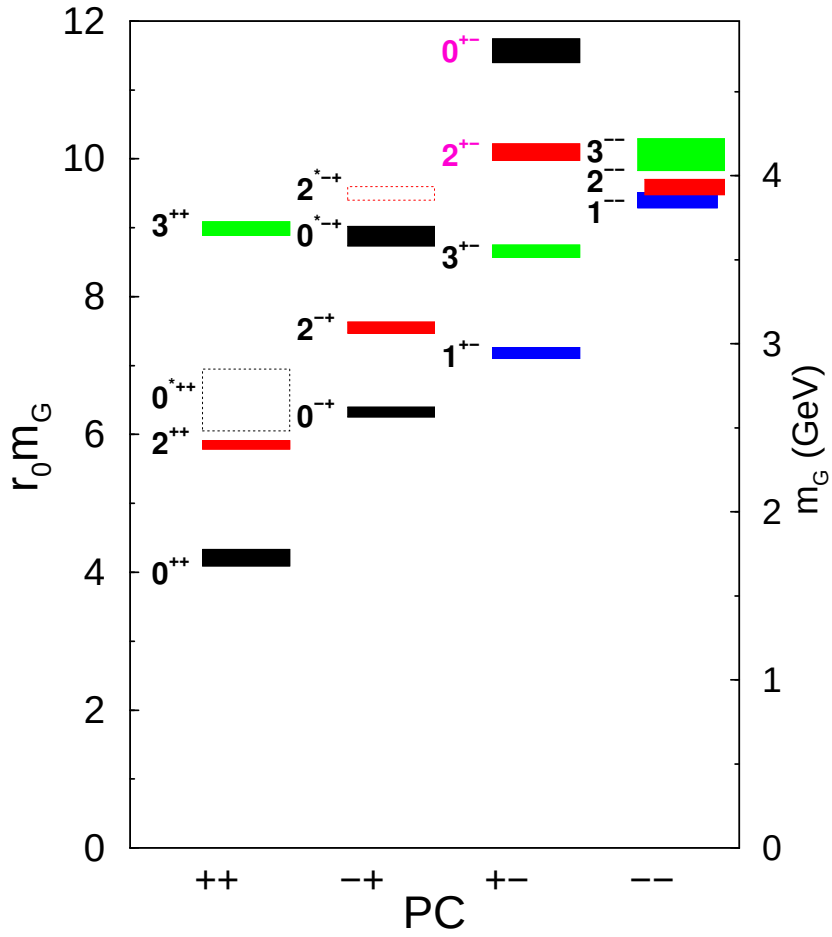

Figure 6: The glueball spectrum from an anisotropic lattice study [33]

a scalar state, at about 1730 MeV; followed by a tensor and pseudoscalar glueball with masses of 2300 and 2350 MeV, respectively. The uncertainty of these calculations is estimated to be of the order of 100 MeV. These masses are supported by other models, bag models [13], flux tubes [16], or QCD sum rules [34]. In publications on bag model calculations, rather low glueball

masses were quoted since the $\eta(1440)$ was identified as pseudoscalar glueball and was used as a mass scale.

The low-lying glueballs all have quantum numbers which allow mixing with conventional mesons. Hence you should expect mixing between glueballs and $q\bar{q}$ mesons. The glueball strength is then diluted over two or more physical states. This is very difficult to establish (unless you impose the existence of a glueball right from the beginning), and even more difficult to rule out.

Glueballs are compact objects. The size of the ground state is predicted to be smaller than that of $q\bar{q}$ mesons, ~ 0.5fm or smaller.

3.1.2 Hints for glueball hunters

Glueballs are supposed to be produced preferentially in gluon-rich processes like, e.g., radiative J/Ψ decays. The J/Ψ is narrow: the OZI rule suppresses decays of the $c\bar{c}$ system into light quarks and the $D\bar{D}$ threshold is far above the mass of the J/Ψ. In most decays the J/Ψ undergoes a transition into 3 gluons which then convert into hadrons. But the J/Ψ can also decay into 2 gluons and a photon. The 2 gluons can interact and must form glueballs - if they exist.

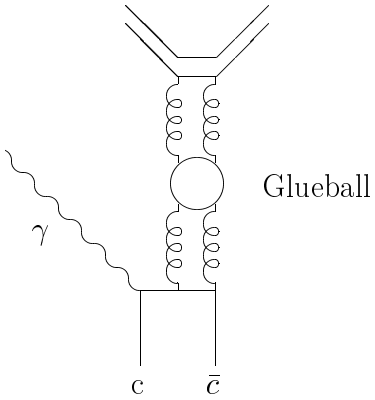

Central production is another process in which glueball should be produced abundantly. In central production two hadrons pass by each other 'nearly untouched' and are scattered diffractively in forward direction. No valence quarks are exchanged. Therefore this process is often called Pomeron-Pomeron scattering. The absence of valence quarks in the production process makes central production a good place to search for glueballs.

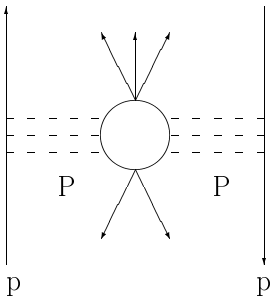

Finally, one can argue that in $\bar{p}p$ annihilation quark-antiquark pairs annihilate into gluons, they will interact and may form glueballs. In any case, any glueball decays into hadrons and hence hadroproduction of glueballs must be possible. Hadroproduction experiments have the advantage - compared to J/Ψ decays - that much higher statistics can be collected.

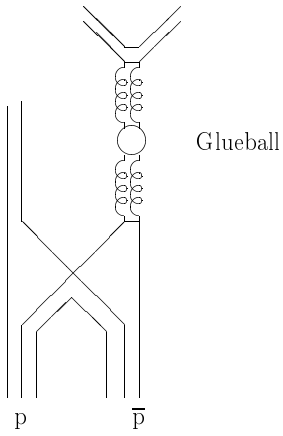

A further distinctive property of glueballs is their decay. Being a flavor singlet, glueballs should decay with flavor symmetry: thus the decay into $\pi\pi$, $\eta\eta$, $\eta\eta'$ and $K\bar{K}$ should scale as $3:1:0:4$, after correcting for phase space. As we have seen, η and η' mesons may be gluish, and SU(3) symmetry could be broken in favor of decays into these two mesons. Also glueball-$q\bar{q}$ mixing will destroy this simple pattern. A detailed and still useful account of early suggestions how to search for glueballs and how to identify them can be found in [35].

3.2 Scalar mesons and the Crystal Barrel experiment at LEAR

Our knowledge on scalar mesons was greatly improved when the data from the Crystal Barrel experiment were analyzed. The Crystal Barrel detector was one of the experimental installations at LEAR; its most prominent feature are 1380 CsI crystals surrounding a H_2 or D_2 target all pointing at the target center, with a solid angle coverage of 98% of 4π. The shape of the detector - a barrel - was chosen to house a vertex detector and an inner drift chamber for charged particle reconstruction. The results and analysis methods are reviewed in detail by Amsler [36].

3.2.1 The life history of antiprotons

Antiprotons annihilating in H_2 or D_2 undergo a series of processes which are very relevant for the annihilation process. Therefore we review shortly the capture process and the atomic cascade which precedes annihilation. We use H_2 as example.

Antiprotons stopping in hydrogen are captured in the Coulomb field of a proton by Auger emission of an electron (or chemical dissociation of H_2 and subsequent internal Auger effect) thus forming antiprotonic hydrogen atoms.

Four processes are important: Auger ejection of electron from neighboring hydrogen atoms, transitions between states with different angular momenta l but identical principal quantum number n due to Stark mixing in the presence of strong electric fields, radiative transitions to lower levels, and annihilation. Obviously the first two processes are density dependent. At the density of liquid H_2, they play a very important role. The Stark effect mixes the angular momentum with the effect that $\sim$90% of all antiprotons annihilate from high-n S states of the $\bar{p}p$ atom. At lower density, e.g. in H_2 gas, Stark mixing rates are smaller and the chance increases that $\bar{p}p$ atoms in P states live long enough to annihilate before the next collision occurs: at atmospheric pressure the chances for S and P capture are about equal. In low-pressure gas, Stark mixing and Auger rates are sufficiently slow to allow radiative transitions to the $2P$ level from which then P-state capture predominates (99%). The strong interaction is weak in D levels and no annihilation occurs from those levels. The processes are depicted in Fig. 7. A review of the field of antiprotonic hydrogen atoms can be found in [37].

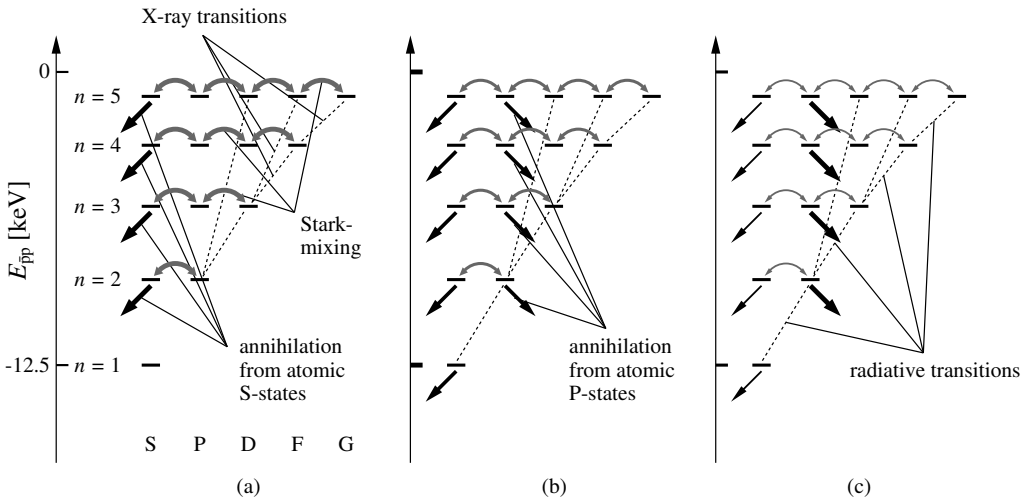

Figure 7: Processes contributing to the cascade of antiprotonic hydrogen atoms, see text.

3.2.2 Quantum numbers of the $\bar{p}p$ system

Proton and antiproton both carry isospin $|I, I_3 >= |\frac{1}{2}, \pm\frac{1}{2} >$. The two isospin couple to $|I = 0, I_3 >= 0$ or $|I = 1, I_3 >= 0$ with $I_3 = 0$ In the absence of initial state interactions between proton and antiproton the

relation

$$\bar{\mathrm{p}}\mathrm{p} = \sqrt{\frac{1}{2}}\left(|\mathrm{I}{=}1, \mathrm{I}_3 = 0 > + |\mathrm{I}{=}0, \mathrm{I}_3 = 0 >\right).$$

holds. One could expect processes of the type $\bar{\mathrm{p}}\mathrm{p} \to \bar{\mathrm{n}}\mathrm{n}$ in the initial state but charge exchange - which would lead to unequal weight of the two isospin components - seems to be not very important [38].

The quantum numbers of the $\bar{\mathrm{p}}\mathrm{p}$ system are of course the same as those for $q\bar{q}$ systems; both are bound states of fermion and anti-fermion. Since isospin can be I=0 or I=1, every atomic $\bar{\mathrm{p}}\mathrm{p}$ state may have G-parity +1 or -1. Table 2 lists the quantum numbers of atomic levels from which annihilation may occur. The $\bar{\mathrm{p}}\mathrm{n}$ system has always I=1, every second level in the Table does not exist. For annihilation into specific final states, selection rules may restrict the number of initial states. Annihilation into any number of π^0 and η mesons is e.g. allowed only from positive-parity states.

$^{2S+1}L_J$	$I^G\left(J^{PC}\right)$	
$^1S_0$	$1^-(0^{-+})$	$0^+(0^{-+})$
$^3S_1$	$1^+(1^{--})$	$0^-(1^{--})$
$^1P_1$	$1^+(1^{+-})$	$0^-(1^{+-})$
$^3P_0$	$1^-(0^{++})$	$0^+(0^{++})$
$^3P_1$	$1^-(1^{++})$	$0^+(1^{++})$
$^3P_2$	$1^-(2^{++})$	$0^+(2^{++})$

Table 2: Quantum numbers of levels of the $\bar{\mathrm{p}}\mathrm{p}$ atom from which annihilation may occur.

3.2.3 The Dalitz plot

In a process in which the initial $\bar{\mathrm{p}}\mathrm{p}$ atom annihilates into three particles, the full dynamics can be visualized in a Dalitz plot. The three final-state particles have totally 12 components of four-vectors. Their masses are known, the orientation in space is irrelevant for understanding the process (the orientation is given by 3 Euler angles); energy and momentum conservation provides 4 constraints. Hence 2 variables are sufficient to describe the full event. The two variables are often chosen as two (squared) invariant masses

of two convenient pairs of the 3 final-state particles, $M^2_{1,2}$ and $M^2_{1,3}$ where the squared invariant masses are calculated from the momenta of the particles:

$$M^2_{ij} = (p_i + p_j)^2 = (E_i + E_j)^2 - (\vec{p_i} + \vec{p_j})^2$$

The density distribution in a two-dimensional histogram $M^2_{1,2}$ versus $M^2_{1,3}$ is called Dalitz plot.

The following equation holds:

$$m^2_{12} + m^2_{23} + m^2_{13} = M^2 + m^2_1 + m^2_2 + m^2_3$$

M is the mass of the $\bar{\text{p}}$p atom, m_i are the masses of the final-state particles and $\vec{P}$ is the 3-momentum of the initial-state (for $\bar{\text{p}}$p-annihilation at rest $\vec{P} = 0$). A particular simple Dalitz plot is depicted in Fig. 8. It represents the reaction $\bar{\text{p}}\text{p} \to \pi^+\pi^-\pi^0$.

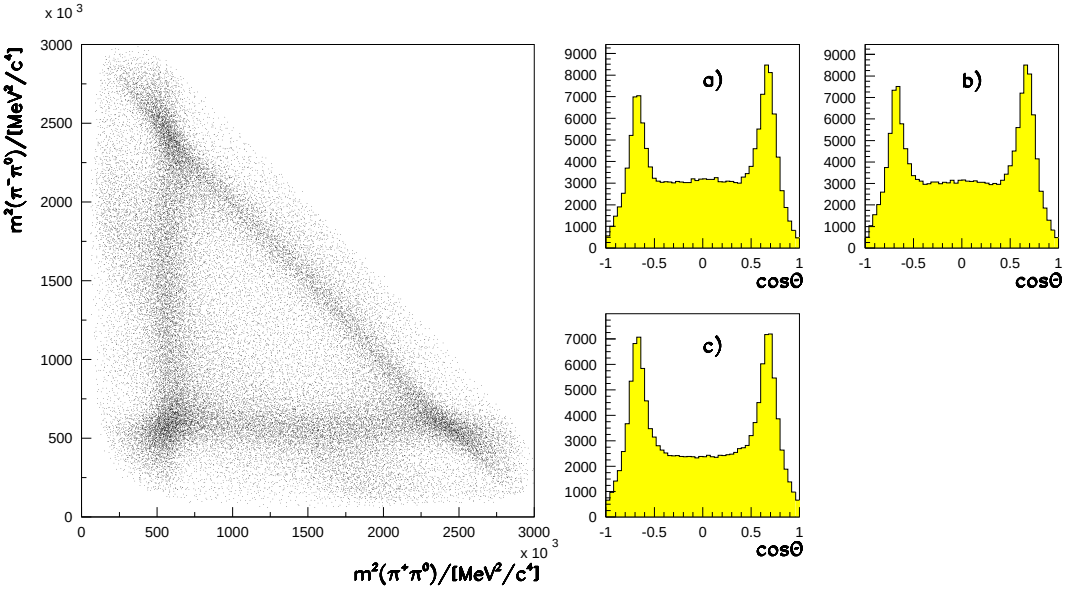

Figure 8: The $\pi^+\pi^-\pi^0$ Dalitz plot in $\bar{\text{p}}$p annihilation at rest, and ρ^+ (a), ρ^- (b) and ρ^0 (c) decay angular distributions.

A resonance in the subsystem of particle π^+ and π^0 ($=\rho^+$) gives an accumulation along a vertical line, a $\pi^-\pi^0$ resonance ($=\rho^-$) is seen as enhancement in horizontal direction, a $\pi^+\pi^-$ resonance ($=\rho^0$) is observed as accumulation along the second diagonal.

The intensity distribution along the ρ^+ band gives directly the $\rho^+ \to \pi^+\pi^0$ angular distribution in the ρ^+ rest system (as a function of $\cos\theta_{\pi^+\pi^0}$). Care

has to be taken because of interferences; the ρ^+ and ρ^- bands cross in the lower left corner of the Dalitz plot. The amplitudes for the two processes $\bar{p}p \to \rho^+\pi^-$ and $\bar{p}p \to \rho^-\pi^+$ interfere constructively and lead to marked deviations of the observed angular distribution from the expected one. This can be appreciated by looking at the angular distributions in Fig. 8. The $\rho^+ \to \pi^+\pi^0$ distribution follows $\sin^2\Theta$ when annihilation precedes from the isospin zero component in the $^3S_1$ initial state. The crossings of the ρ^+ band with the ρ^- and ρ^0 bands leads to an increase of the intensity by a factor 4 because of quantum mechanical interference (the amplitudes are added!). The increase of intensity in the $\rho^\pm$ - ρ^0 crossing is slightly smaller than for the ρ^+ - ρ^- crossing. This is due to a small contribution from the isovector part of the $^1S_0$ state of the $\bar{p}p$ atom. From this initial $\bar{p}p$ state, annihilation into $\rho^0\pi^0$ is forbidden, the $\rho^\pm$ decay angular distribution follows $\cos^2\Theta$. The $\sin^2\Theta$ and $\cos^2\Theta$ parts contribute a small constant distribution which is clearly seen in the data. The measured constant fractions in Fig. 8a,b,c are larger than estimated from the difference in $\rho^\pm$ and ρ^0 intensities: this is due to annihilation from the $^1P_1$ state. A partial wave analysis identifies these observations, determines masses and widths of contributing resonances and gives fractional contributions from $\bar{p}p$ initial states given in Table 2 to the $\pi^+\pi^-\pi^0$ final state.

3.2.4 The $f_0(1500)$ in Crystal Barrel Dalitz plots

We now show the four Dalitz plots from which main properties of the $f_0(1370)$ and $f_0(1500)$ are derived. These two states were discovered by the Crystal Barrel Collaboration; both play an eminent role in the present glueball discussion. The Dalitz plots - Fig. 9 - stem from four publications of the Crystal Barrel Collaboration [39]-[42] . In the $3\pi^0$ (upper left) and the $\pi^0 2\eta$ (upper right) Dalitz plots the $f_0(1500)$ is clearly seen as band structure. In $\pi^0\eta\eta'$ a strong threshold enhancement in the $\eta\eta'$ invariant mass is seen (lower left); the final state $K_l K_l \pi^0$ has prominent K^* bands; their interference with the $f_0(1500)$ makes the intensity so large in the left corner of the Dalitz plot (lower right).

The reactions $\bar{p}p \to \pi^+\pi^- 3\pi^0$ [43], $\bar{p}p \to 5\pi^0$ [44], $\bar{p}n \to \pi^- 4\pi^0$ [45] and $\bar{p}n \to \pi^- 2\pi^- 2\pi^0\pi^+$ [46] were studied to determine decays into 4 pions.

3.2.5 Scalar mesons

We have seen that decays of mesons are constrained by SU(3) relations. So there is hope that the glueball nature of a state can be un-revealed by

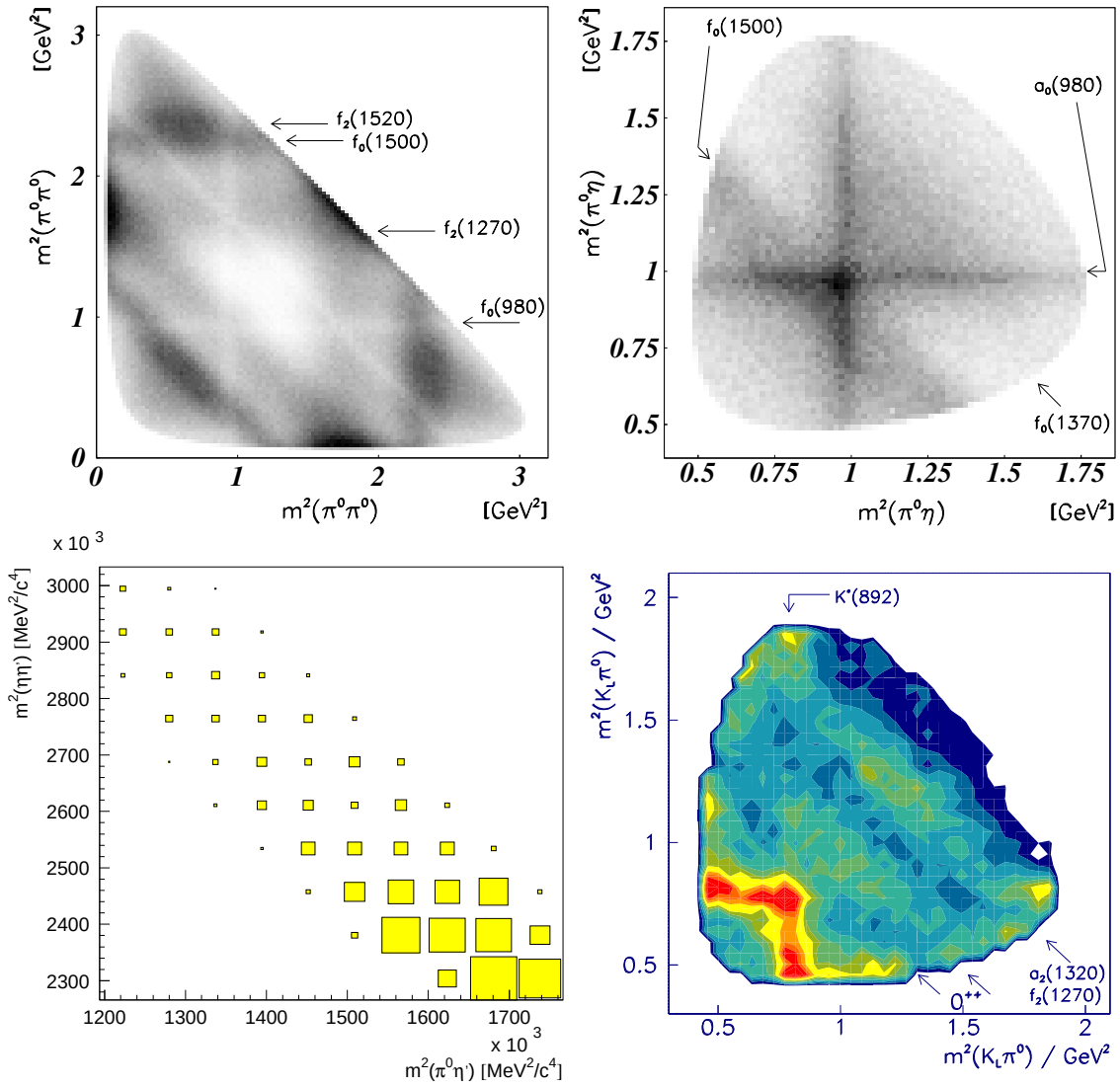

Figure 9: Dalitz plots for $\bar{\mathrm{p}}\mathrm{p}$ annihilation at rest into $3\pi^0$ (upper left), $\pi^0 2\eta$ (upper right), $\pi^0\eta\eta'$ (lower left), $\mathrm{K}_l\mathrm{K}_l\pi^0$ (lower right). The $f_0(1370)$ contributes to (a,b,d), the $f_0(1500)$ to all 4 reactions. The $\mathrm{K}_l\mathrm{K}_l\pi^0$ is difficult to interprete in the black-and-white version; the colored Dalitz plot can be found on the web. The data are from [39]-[42].

inspecting the coupling to various final states. Table 3 lists partial widths of the $f_0(1370)$ and $f_0(1500)$ as derived from the Crystal Barrel Collaboration. Most striking is the similarity of the partial decay widths for the decays into $\eta\eta$ and $\eta\eta'$ and the smallness of the $\mathrm{K\bar{K}}$ coupling of the $f_0(1500)$. (Remember that we expect ratios for $\pi\pi : \eta\eta : \eta\eta' : \mathrm{K\bar{K}}$ of $3:1:0:4$, after removal of phase

	$f_0(1370)$	$f_0(1500)$
Γ_{tot}	275 ± 55	130 ± 30
$\Gamma_{\sigma\sigma}$	120.5 ± 45.2	18.6 ± 12.5
$\Gamma_{\rho\rho}$	62.2 ± 28.8	8.9 ± 8.2
$\Gamma_{\pi^*\pi}$	41.6 ± 22.0	35.5 ± 29.2
$\Gamma_{a_1\pi}$	14.10 ± 7.2	8.6 ± 6.6
$\Gamma_{\pi\pi}$	21.7 ± 9.9	44.1 ± 15.4
$\Gamma_{\eta\eta}$	0.41 ± 0.27	3.4 ± 1.2
$\Gamma_{\eta\eta'}$		2.9 ± 1.0
$\Gamma_{\bar{K}K}$	(7.9 ± 2.7) to (21.2 ± 7.2)	8.1 ± 2.8

Table 3: Partial decay widths of the $f_0(1370)$ and $f_0(1500)$ from Crystal Barrel data

space). Obviously, the $f_0(1500)$ cannot be a pure glueball, it must mix with nearby states! The $f_0(1370)$ has important couplings to two pairs of π^0-mesons, to $\sigma\sigma$. This is evident from Fig. 10.

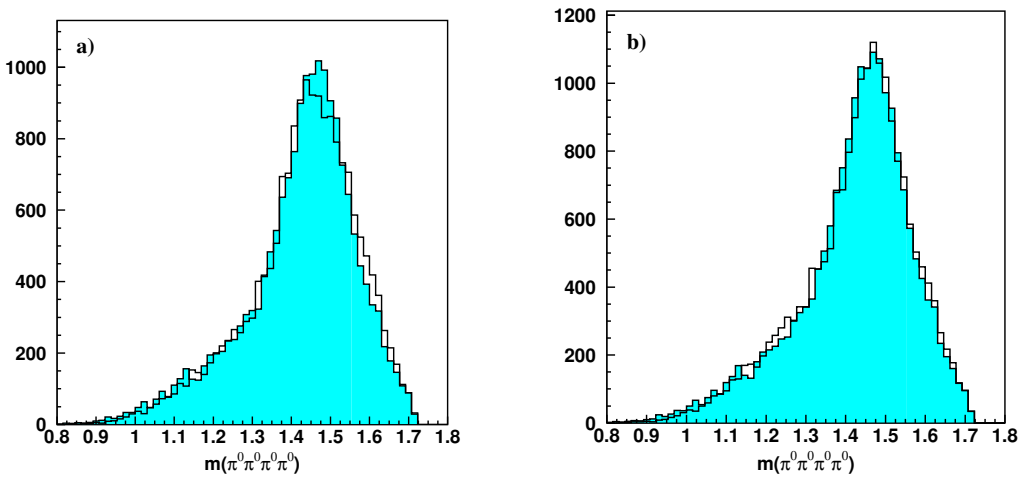

Figure 10: The $4\pi^0$ invariant mass in the reaction $\bar{p}n \to \pi^- 4\pi^0$. A fit (including other amplitudes) with one scalar state fails; two scalar resonances at 1370 and 1500 MeV give a good fit. Note that the full 8-dimensional phase space is fitted and not just the mass projection shown here; (from [45]).

3.3 Scalar mesons and the scalar glueball

3.3.1 Established scalar mesons

Below 2 GeV, 15 'established' scalar mesons are listed by the Particle Data Group [29] which are shown in the Table below.

I = 1/2	I = 1	I = 0
		$f_0(400-1200)$
	$a_0(980)$	$f_0(980)$
		$f_0(1370)$
$K_0^*(1430)$	$a_0(1490)$	$f_0(1500)$
		$f_0(1710)$

The lowest-mass entry is an $f_0(400-1200)$ representing the scalar isoscalar $\pi\pi$ interactions, often called σ-meson. For reasons discussed below, it is likely not a $q\bar{q}$ meson. The two states at the $K\bar{K}$ threshold, the $f_0(980)$ and the $a_0(980)$, have a large coupling to $K\bar{K}$ and a comparatively narrow width. Hence they are often discussed as $K\bar{K}$ molecules [47] or as four-quark states [48] and not as $q\bar{q}$ mesons.

Leaving out the 5 states $f_0(400-1200)$, $f_0(980)$ and $a_0^{\pm,0}(980)$, we remain with a decuplet of states and not with nine states as expected in the quark model. The three scalar isoscalar states $f_0(1370)$, $f_0(1500)$ and $f_0(1750)$ cannot possibly belong to the same nonet. Since the $f_0(1370)$ is a $u\bar{u}+d\bar{d}$ state (it decays only weakly into $K\bar{K}$) we expect ideal mixing and an $s\bar{s}$state at 1620 MeV, not too far from the observed $f_0(1710)$. This line of argument is the basis for the assignment by the Particle Data Group [29] of the $f_0(1370)$ and $f_0(1710)$ to the 1^3P_0 nonet. The $f_0(1500)$ is discussed as glueball candidate.

3.3.2 Meson-glueball mixing

Several authors have suggested scenarios in which a scalar glueball mixes with two $q\bar{q}$ states [53]-[58]. The mixing angles were (partly) determined from partial decay widths of the scalar states. Only M. Strohmeier-Presicek *et al.* [58] includes the 4π decays into the analysis. You may start your mixing scheme by assuming that the 'primordial' glueball is in between a low-mass $u\bar{u}+d\bar{d}$ and the high-mass $s\bar{s}$state [53, 56], or by assuming that the primordial glueball is above both states [54]. These two options lead to different mixing schemes. Some of them are listed in Table 4. Not shown in the Table is the mixing scenario suggested by Narison [34] who finds that all three states share the glueball in approximately equal portions. Anisovich et al. [59] believe 5 states to exist below 1.8 GeV. They develop from the 1^3P_0 and 2^3P_0 $q\bar{q}$ states and the scalar glueball. Through mixing the glueball strength distributes between the $f_0(1370)$ and $f_0(1500)$ and a broad underlying component. SU(3) symmetry in the decays of $^3P_0$ $q\bar{q}$ states is imposed in the fits as well as flavor-blindness of the primordial glueball.

3.3.3 The scalar glueball

All mixing schemes agree in that the scalar glueball manifests itself in the scalar meson sector and that it has a mass, before mixing, of about 1600 MeV. Hence all authors agree that lattice gauge theories are doing well in predicting a scalar glueball at this mass. The mixing schemes disagree how the glueball is distributed between the three experimentally observed states. Some of the models assign very large $s\bar{s}$components to the $f_0(1370)$ or $f_0(1500)$; this is certainly not compatible with data.

4 Scrutinizing the scalar glueball

The interpretation of two resonances, of the $f_0(980)$ and the $f_0(1370)$, plays a decisive role in the meson-glueball mixing scenarios. Also, the nature of the $f_0(400-1200)$ is unclear. We discuss these 3 states in some detail.

4.1 Scalar mesons below 1.3 GeV

4.1.1 The scalar isoscalar $\pi\pi$ interactions

The S-wave $\pi\pi$ interactions at small energies are elastic. The T-matrix saturates unitarity, the inelasticity parameter $\eta_{l=0}$ vanishes. Inelastic channels

Amsler and Close [53]							
$f_0(1370)$	=	$0.86\frac{1}{\sqrt{2}}(u\bar{u}+d\bar{d})$	+	$0.13\ s\bar{s}$	-	0.50	glueball
$f_0(1500)$	=	$0.43\frac{1}{\sqrt{2}}(u\bar{u}+d\bar{d})$	-	$0.61\ s\bar{s}$	+	$\underline{0.61}$	glueball
$f_0(1750)$	=	$0.22\frac{1}{\sqrt{2}}(u\bar{u}+d\bar{d})$	-	$0.76\ s\bar{s}$	+	$\underline{0.60}$	glueball
Lee and Weingarten [54]							
$f_0(1370)$	=	$0.87\frac{1}{\sqrt{2}}(u\bar{u}+d\bar{d})$	+	$0.25\ s\bar{s}$	-	0.43	glueball
$f_0(1500)$	=	$-0.36\frac{1}{\sqrt{2}}(u\bar{u}+d\bar{d})$	+	$0.91\ s\bar{s}$	-	0.22	glueball
$f_0(1750)$	=	$0.34\frac{1}{\sqrt{2}}(u\bar{u}+d\bar{d})$	+	$0.33\ s\bar{s}$	+	$\underline{0.88}$	glueball
De-Min Li *et al.*[55]							
$f_0(1370)$	=	$-0.30\frac{1}{\sqrt{2}}(u\bar{u}+d\bar{d})$	-	$0.82\ s\bar{s}$	+	0.49	glueball
$f_0(1500)$	=	$+0.72\frac{1}{\sqrt{2}}(u\bar{u}+d\bar{d})$	-	$0.53\ s\bar{s}$	-	0.45	glueball
$f_0(1750)$	=	$+0.63\frac{1}{\sqrt{2}}(u\bar{u}+d\bar{d})$	+	$0.22\ s\bar{s}$	+	$\underline{0.75}$	glueball
Close and Kirk [56]							
$f_0(1370)$	=	$-0.79\frac{1}{\sqrt{2}}(u\bar{u}+d\bar{d})$	-	$0.13\ s\bar{s}$	+	0.60	glueball
$f_0(1500)$	=	$-0.62\frac{1}{\sqrt{2}}(u\bar{u}+d\bar{d})$	+	$0.37\ s\bar{s}$	-	$\underline{0.69}$	glueball
$f_0(1750)$	=	$0.14\frac{1}{\sqrt{2}}(u\bar{u}+d\bar{d})$	+	$0.91\ s\bar{s}$	+	0.39	glueball
Celenza *et al.*[57]							
$f_0(1370)$	=	$0.01\frac{1}{\sqrt{2}}(u\bar{u}+d\bar{d})$	-	$1.00\ s\bar{s}$	-	0.00	glueball
$f_0(1500)$	=	$0.99\frac{1}{\sqrt{2}}(u\bar{u}+d\bar{d})$	-	$0.11\ s\bar{s}$	+	0.01	glueball
$f_0(1750)$	=	$0.03\frac{1}{\sqrt{2}}(u\bar{u}+d\bar{d})$	+	$0.09\ s\bar{s}$	+	$\underline{0.99}$	glueball
M. Strohmeier-Presicek *et al.*[58]							
$f_0(1370)$	=	$0.94\frac{1}{\sqrt{2}}(u\bar{u}+d\bar{d})$	+	$0.07\ s\bar{s}$	-	0.34	glueball
$f_0(1500)$	=	$0.31\frac{1}{\sqrt{2}}(u\bar{u}+d\bar{d})$	-	$0.58\ s\bar{s}$	+	$\underline{0.75}$	glueball
$f_0(1750)$	=	$0.15\frac{1}{\sqrt{2}}(u\bar{u}+d\bar{d})$	+	$0.81\ s\bar{s}$	+	$\underline{0.57}$	glueball

Table 4: Decomposition of the wave function of 3 scalar isoscalar states into their quarkonium and glueball contribution in various models.

open up at the K$\bar{\text{K}}$ threshold, and at this mass the inelasticity is large. At energies above 1 GeV, the inelasticity is small again. Results from a recent phase shift analysis of π scattering off a polarized target into two pions [61] are shown in Fig. 17. At 980 MeV a dip is observed corresponding to the $f_0(980)$ which has large coupling to K$\bar{\text{K}}$. A second dip is suggested at 1500 MeV corresponding to the $f_0(1500)$. The amplitude reaches maxima at positions which correspond to the old $\sigma(600)$ which plays an important role in one-boson-exchange-potentials, and to the old $\epsilon(1300)$. The dips are associated with additional rapid phase motions. The background amplitude and its phase motion are correctly reproduced by t-channel ρ exchange [49, 50].

Adding further t-channel amplitudes for ω, Φ and K* exchange, Speth and collaborators describe both the $f_0(980)$ and the $a_0(980)$ as generated by t-channel exchange dynamics [51] with the K$\bar{\text{K}}$ system forming a bound state in isoscalar but not in isovector interactions. Related is the interpretation of these two resonances at the K$\bar{\text{K}}$ threshold as K$\bar{\text{K}}$ molecules [47]. These states can also be understood as $q\bar{q}$ mesons with properties governed by the K$\bar{\text{K}}$ threshold [52]. And they are discussed as $q\bar{q}\bar{q}$ resonances [48, 62].

4.1.2 The $f_0(980)$ and $a_0(980)$ in Z^0 fragmentation

At LEP the fragmentation of quark- and gluon jets has been studied intensively [63]. In particular the inclusive production of the $f_0(980)$ and $a_0(980)$ provides new insight into their internal structure. The OPAL collaboration searched for these and other light meson resonances in a data sample of 4.3 million hadronic Z^0 decays. For the $f_0(980)$ a coupled channel analysis was made by simultaneously fitting the inclusive $\pi\pi$ and K$\bar{\text{K}}$ mass spectra. Some total inclusive rates are listed in Table 5. We notice that the three mesons η', $f_0(980)$ and $a_0(980)$ - which have very similar masses - also have production rates which are nearly identical (the two charge modes of the $a_0(980)^{\pm}$ need to be taken into account). Hence there is primary evidence that the three mesons have the same internal structure, that they are all three $q\bar{q}$ states.

This conclusion can be substantiated by further studies [64]. The production characteristics of the $f_0(980)$ are compared to those of $\text{f}_2(1270)$ and $\Phi(1020)$ mesons, and with the Lund string model of hadronization within which the $f_0(980)$ is treated as a conventional meson. No difference is observed in any of these comparisons between the $f_0(980)$ and the $\text{f}_2(1270)$ and $\Phi(1020)$. We emphasize that it would be extremely useful if the studies could be extended to include other scalar particles. Of course, background problems become more important for higher-mass particles and their production is reduced.

π^0	$9.55 \pm 0.06 \pm 0.75$
η	$0.97 \pm 0.03 \pm 0.11$
η'	$0.14 \pm 0.01 \pm 0.02$
$a_0^{\pm}(980)$	$0.27 \pm 0.04 \pm 0.10$
$f_0(980)$	$0.141 \pm 0.007 \pm 0.011$
$\Phi(1020)$	$0.091 \pm 0.002 \pm 0.003$
$f_2(1270)$	$0.155 \pm 0.011 \pm 0.018$

Table 5: Yield of light mesons per hadronic Z^0 decay; (from [63],[64]).

4.1.3 The two-photon widths of the $f_0(980)$ and $a_0(980)$

In a recent report, Boglione and Pennington [65] reexamined data on two-photon production of scalar mesons. The experimental information from different experiments is sometimes inconsistent resulting in large errors. On the other hand, two-photon decays provide deep insight into the internal structure [66]. The ratio [29]

$$R_{\gamma\gamma} = \frac{\Gamma_{f_0(980)\to\gamma\gamma}}{\Gamma_{a_0(980)\to\gamma\gamma}} = 1.38 \pm 0.63 \tag{2}$$

is related to the scalar mixing angle (with $f_0(980)$ being the singlet for $\Theta = 0$) by

$$R_{\gamma\gamma} = \frac{1}{3} \cdot \left(\sin\Theta + 3\sqrt{2} \cdot \cos\Theta\right)^2 \tag{3}$$

There are two solutions: $\Theta = (66.8 \pm 15)^\circ$ and $\Theta = (-27.4 \pm 15)^\circ$. Only the latter value is compatible with the result obtained in [66]. The angle $\Theta = 60^\circ$ corresponds to a wave function

$$f_0(980) \sim \sqrt{\frac{1}{9}}\frac{1}{\sqrt{2}}(u\bar{u} + d\bar{d}) + \sqrt{\frac{8}{9}}s\bar{s} \tag{4}$$

which has a larger $s\bar{s}$content than a isosinglet state would have, likely due to a strong K$\bar{\text{K}}$ component in the wave function.

4.1.4 The $\Phi\to\gamma f_0(980)$ decay

The Φ radiative decay rate into the $f_0(980)$ is surprisingly large [67],

$$\frac{\Gamma_{\Phi\to\gamma f_0(980)}}{\Gamma_{\Phi\text{tot}}} = (3.5 \pm 0.3^{+0.8}_{-0.3}) \cdot 10^{-4} \tag{5}$$

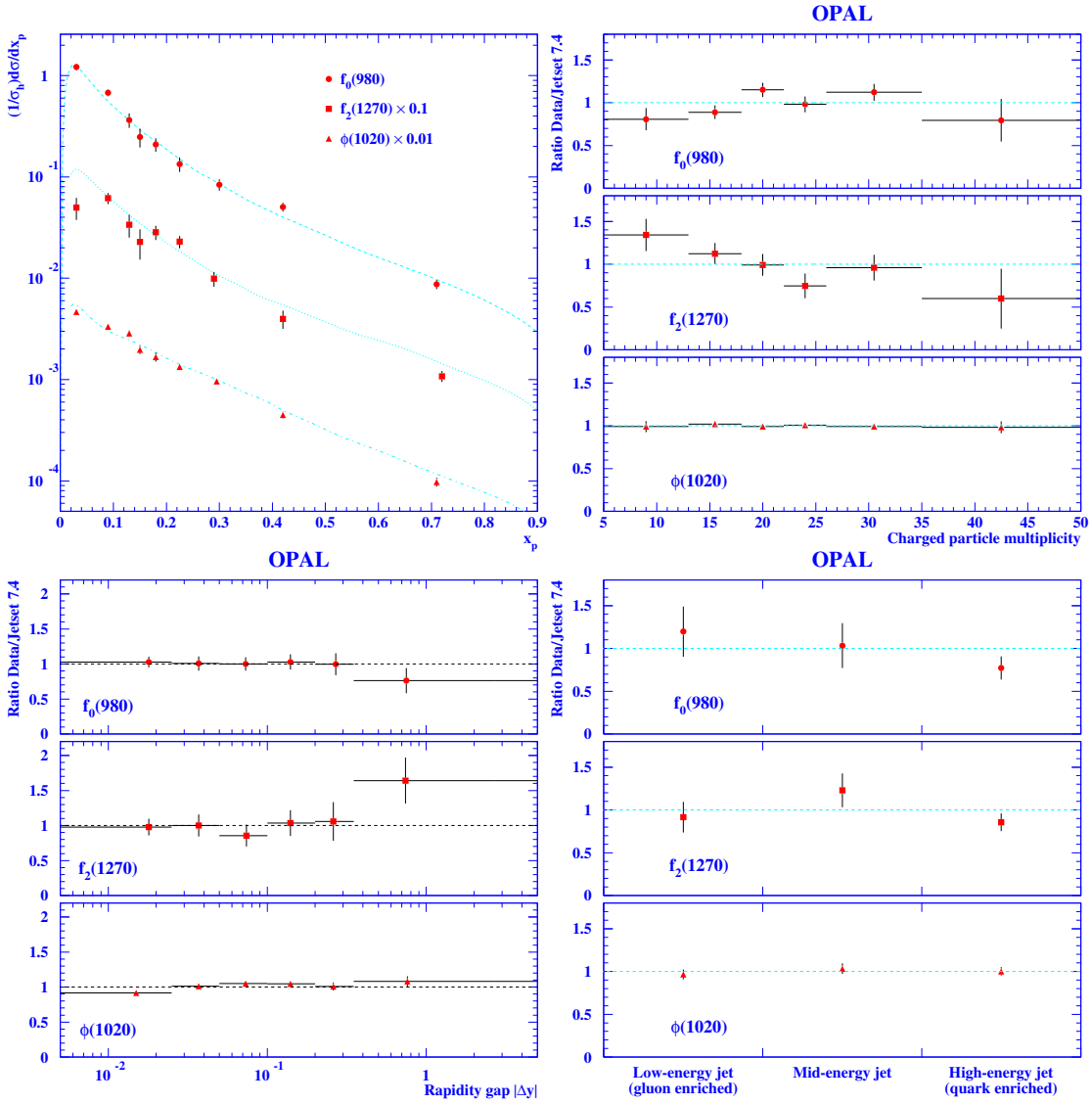

Figure 11: Fragmentation of Z^0's into jets containing $f_0(980)$, $f_2(1270)$ and $\Phi(1020)$ mesons as functions of x_p (a), of the charged-particle multiplicity (b), of the rapidity gap between the meson and the nearest charged particle (c) and of the jet energy (d). The lines correspond to simulations [64] based on the Lund string model of hadronization.

Early predictions [68] assuming different structures for the $f_0(980)$, $q\bar{q}$, $K\bar{K}$ or four-quark, were all well below the recent experimental value [67]. Recently, the reaction was studied by Markushin [69] and by Marco *et al.* [70]. They found that kaonic loops play a decisive role and that, including these, rate and $\pi\pi$ invariant mass distributions are well reproduced. The $f_0(980)$ resonance corresponds to a T-matrix pole close to the $K\bar{K}$ threshold; a good description of the data is achieved assuming that the pole is of dynamical origin and

represents a molecular-like $K\bar{K}$ state. An underlying $q\bar{q}$ component is possible but not required.

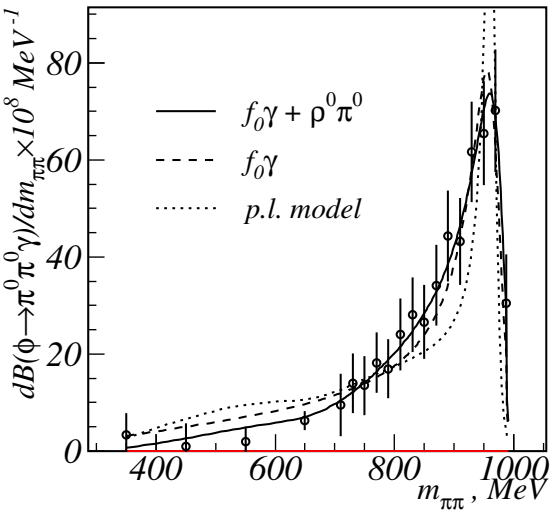

Figure 12: The $\pi\pi$ invariant mass distribution from $\Phi\to\pi\pi\gamma$. The fit assumes that the $f_0(980)$ is a four-quark state; (from [67]). Other models give similar agreement between data and fit.

The rate for $\Phi\to\gamma a_0(980)$ is smaller by a factor ~ 4 [71] than the rate for $\Phi\to\gamma f_0(980)$ which seems difficult to reproduce if both mesons are $K\bar{K}$ molecules. In this case their rates should be equal [68]. If the $f_0(980)$ has a structure as given in (4) and the $a_0(980)$ is $\frac{1}{\sqrt{2}}(u\bar{u} - d\bar{d})$, the decay chain $\Phi\to\gamma f_0(980); f_0(980)\to\pi\pi$ should be much larger than $\Phi\to\gamma a_0(980); a_0(980)\to\eta\pi$. The data are in-between these two extreme values. This may suggest that both pictures are oversimplified. Isospin-breaking mixing between $f_0(980)$ and $a_0(980)$ due to the mass splitting between the K^+K^- and $K^0\bar{K}^0$ thresholds [72],[73] are too weak to be responsible for the large $\Phi\to\gamma a_0(980)$ rate.

4.1.5 D_s decays into three pions

D_s decays into three pions provide further insight into the spectrum of isoscalar scalar resonances. The comparatively large rate for three-pion production is surprising: consider the reaction $D_s^+\to 2\pi^+\pi^-$. The quark content of the D_s^+ is $c\bar{s}$. In the decay, the c undergoes a transition to an s, the W^+ converts into a π^+. Hence an $s\bar{s}$ state is produced which decays into $\pi^+\pi^-$. This is OZI rule violating, and the OZI violation is strong:

$$\frac{\Gamma_{\pi^+\pi^-\pi^0}}{\Gamma_{K^+K^-\pi^0}} = 0.23 \pm 0.04 \qquad (6)$$

The three-pion Dalitz plot has moderate statistics only, but the $f_0(980)$ is clearly seen and the partial wave analysis finds a second scalar state at

$f_0(1470)$ which we identify with the $f_0(1500)$. The two states $f_0(980)$ and $f_0(1500)$ then both decay into $\pi^+\pi^-$. The data are shown in Fig. 13.

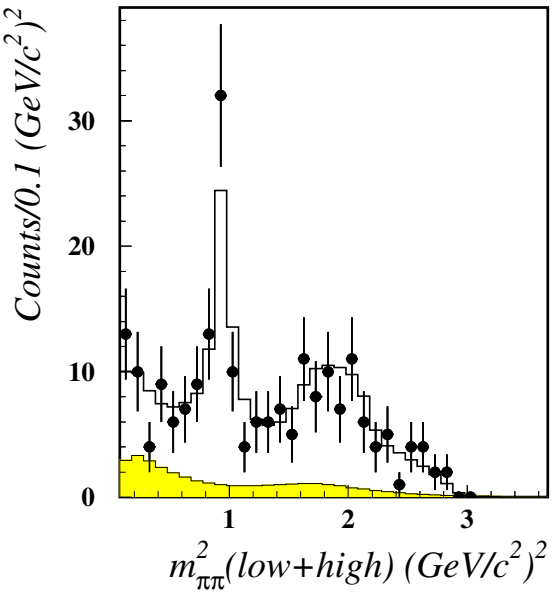

Figure 13: Dalitz plot for OZI violating D_s decays into three pions. The low-mass peak is due to the $f_0(980)$ decaying into $\pi^+\pi^-$, the broad enhancement is assigned to the $f_0(1500)$ (in a partial wave analysis).

We note two aspects: first, the two states $f_0(980)$, $f_0(1500)$ are produced in a similar way and - taking phase space into account - with similar couplings. Second, both mesons do not respect the OZI rule. This is similar to the η and η'. The wave functions of both, $f_0(980)$ and $f_0(1500)$, must contain $u\bar{u} + d\bar{d}$ and $s\bar{s}$ components.

4.1.6 The $f_0(980)$ and $f_0(980)$: $q\bar{q}$ or K$\bar{\text{K}}$?

The situation is confused: when low-energy phenomena are discussed, the K$\bar{\text{K}}$ molecule interpretation provides for a very good description of the data with no $q\bar{q}$ component being required. When you start from the $q\bar{q}$ picture and place a $q\bar{q}$ state in the vicinity of the K$\bar{\text{K}}$ threshold, the state is attracted by the threshold when the coupling to the K$\bar{\text{K}}$ channel is taken into account [74] and a large K$\bar{\text{K}}$ component develops. Reactions like Z^0 fragmentation and D_s decays point at a $q\bar{q}$ nature. We conclude that there are good reasons to believe that the $f_0(980)$ and $a_0(980)$ should be counted as $q\bar{q}$ 1^3P_0 states. Of course, the vicinity of the K$\bar{\text{K}}$ threshold plays a significant role and a large K$\bar{\text{K}}$ component is to be expected as part of their wave functions [52].

4.2 Scalar mesons above 1.3 GeV

4.2.1 D_s decays

D_s decays into three pions show no evidence for the $f_0(1370)$. As discussed, only the two states $f_0(980)$ and $f_0(1500)$ are produced.

4.2.2 The two-photon widths

The Aleph Collaboration searched for two-photon production of the $f_0(1500)$ and the $f_0(1710)$ [75]. No signal was seen. From the absence the authors concluded that

$$\begin{aligned} \Gamma_{\gamma\gamma\to f_0(1500)} \cdot BR(f_0(1500)\to\pi^+\pi^-) < 0.31\text{keV} \\ \Gamma_{\gamma\gamma\to f_0(1710)} \cdot BR(f_0(1710)\to\pi^+\pi^-) < 0.55\text{keV} \end{aligned} \tag{7}$$

at 95% confidence level.

At HADRON97, Barnes estimated that the two-photon width should be of the order of 8 keV. Taken at face value the upper limit in (7) claims that the $q\bar{q}$ content of the $f_0(1500)$ should be at a few % level!

4.2.3 Radiative J/ψ decays

Glueballs have to show up in radiative J/ψ decays. In these decays, one photon and two gluons are emitted by the annihilating $c\bar{c}$ system, the two gluons interact and must form glueballs - if a glueball exists in the accessible mass range. A most prominent - possibly scalar - signal in radiative J/ψ decays into 2η is the old $\Theta(1690)$ with spin 0 or spin 2, which might have a large fraction of glue in its wave function. In a recent reanalysis, the state was shown to be of scalar nature [76]. The scalar part in Fig. 14 shows two resonances, at 1430 MeV and at 1710 MeV. The latter has strong coupling to K$\bar{\text{K}}$. The mass shift from 1500 to 1430 MeV will be discussed below. Three scalar resonances are observed at BES in radiative J/ψ decays into $2\pi^+2\pi^-$ [77]. The results of a partial wave analysis (see Fig. 14) show a slowly rising instrumental background and 3 important contributions with scalar, pseudoscalar and tensor quantum numbers.

Of particular importance here is the scalar part. It is seen to contain 3 resonances, at 1500, 1740 and 2100 MeV. This pattern of states was already suggested in a reanalysis of MARKIII data [78]. The $f_0(1500)$, $f_0(1740)$ and the $f_0(2100)$ have a similar production and decay pattern. Neither a $f_0(1370)$ nor a 'background' intensity is assigned to the scalar isoscalar partial wave.

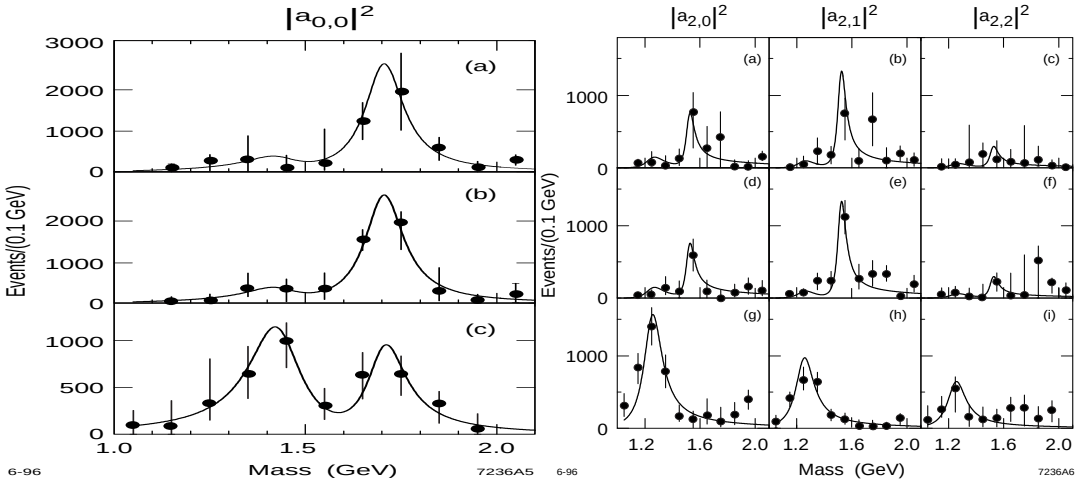

Figure 14: Partial wave analysis of J/ψ radiative decay to two pseudoscalar mesons, from the Mark III collaboration. S-wave (left) and D-wave (right). The top row is the analysis of $J/\psi \to \gamma K_S K_S$, middle row for $J/\psi \to \gamma K^+ K^-$, and bottom row for $J/\psi \to \gamma\pi\pi$. The structure near 1700 MeV/c^2 is clearly dominated by an S-wave state.

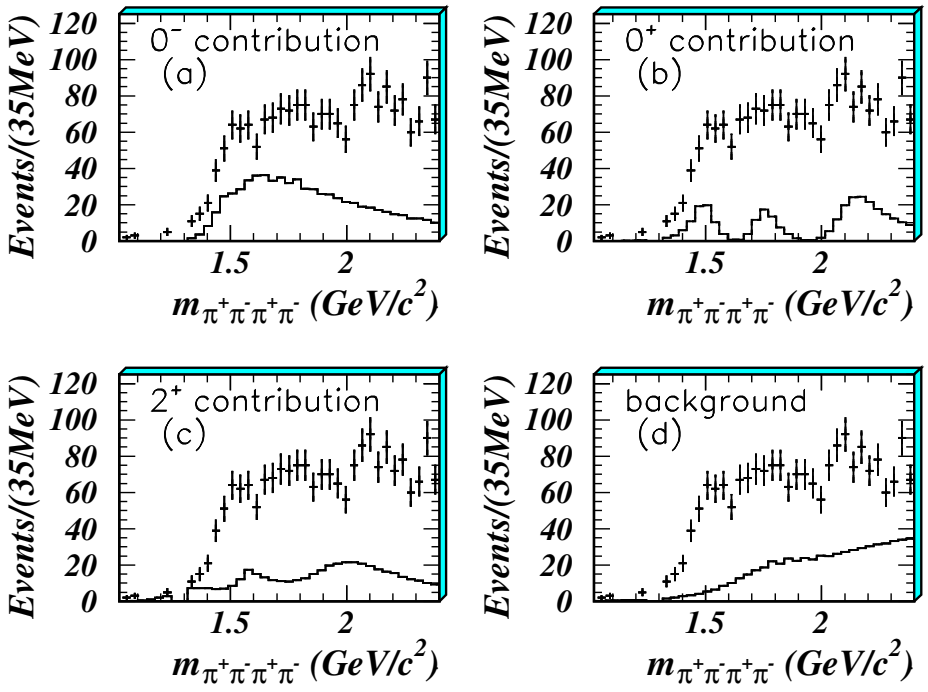

Figure 15: Partial wave decomposition of radiative J/ψ decays into $2\pi^+2\pi^-$ (from [77]).

4.2.4 $\bar{p}p$ annihilation in flight

The $\eta\eta$ invariant mass spectrum produced in $\bar{p}p$ annihilation in flight into $\pi^0\eta\eta$ [79] exhibits three peaks at $f_0(1500)$, $f_0(1750)$ and $f_0(2100)$ MeV, fully compatible with the findings in radiative J/ψ decays into four pions. The data were not decomposed into partial waves in a partial wave analysis, so the peaks could have $J^{PC} = 0^{++}$ or 2^{++}. If the states would have $J^{PC} = 2^{++}$, their decay into $\eta\eta$ would be suppressed by the angular momentum barrier. The fact that the peaks are seen so clearly suggests 0^{++} quantum numbers, and this is the result of the partial wave analysis of the J/ψ data. Hence we believe that the 3 peaks are scalar isoscalar resonances.

4.2.5 Central production

Central production is believed to be a good place for a glueball search. Fig. 16 shows 4π invariant mass spectra from the WA102 experiment [81]. A large peak at 1370 MeV is seen, followed by a dip in the 1500 MeV region and a further (asymmetric) bump.

The partial wave analysis decomposes this structure into several scalar resonances, the $f_0(1370), f_0(1500)$ and $f_0(1750)$ and a new $f_0(1900)$. We note that the partial wave analysis finds $f_0(1370)$ decays into $\rho\rho$ but not into $\sigma\sigma$ while the $f_0(1500)$ shows both decay modes. In the Crystal Barrel experiment the $f_0(1370)$ decays into $\rho\rho$ and into $\sigma\sigma$ with similar strength, see Table 6.

The upper limit for $f_0(1370) \to \sigma\sigma$ of the WA102 experiment is not very restrictive. In the partial wave analysis representing the preferred solution,

$f_0(1370) \to \sigma\sigma / f_0(1370) \to 4\pi$	=	≤ 0.23	WA102
$f_0(1500) \to \sigma\sigma / f_0(1500) \to 4\pi$	=	$0.23 - 0.50$	WA102
$f_0(1370) \to \sigma\sigma / f_0(1370) \to 4\pi$	=	0.51 ± 0.09	CBAR
$f_0(1500) \to \sigma\sigma / f_0(1500) \to 4\pi$	=	0.26 ± 0.07	CBAR

Table 6: Decay fractions into $\sigma\sigma$ of scalar mesons from the WA102 and CBAR experiments.

the upper limit for $f_0(1370) \to \sigma\sigma / f_0(1370) \to 4\pi$ is certainly smaller. On the other hand, in $\bar{p}p$ annihilation the $\sigma\sigma$ decay mode is certainly present and strong. This is an important observation and provides a clue for the

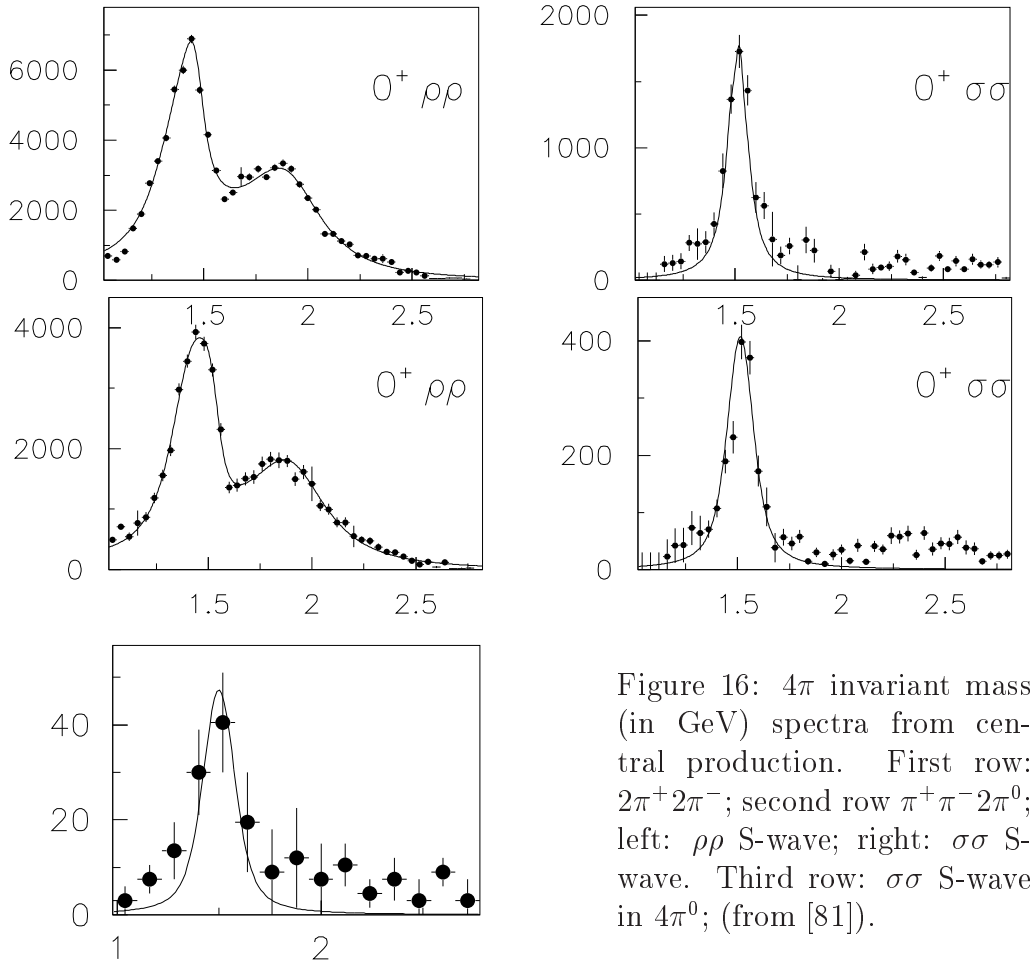

Figure 16: 4π invariant mass (in GeV) spectra from central production. First row: $2\pi^+2\pi^-$; second row $\pi^+\pi^-2\pi^0$; left: $\rho\rho$ S-wave; right: $\sigma\sigma$ S-wave. Third row: $\sigma\sigma$ S-wave in $4\pi^0$; (from [81]).

interpretation of the spectrum of scalar mesons. In any case, there are large differences between the $\rho\rho$ and $\sigma\sigma$ mass distributions which need to be explained.

4.3 The *red dragon* or $f_0(1000)$

Before we continue the discussion we have to introduce a further concept:

4.3.1 s-channel resonances and t-channel exchanges

Fig. 17 shows the $\pi\pi$ scattering amplitude. The phase rises slowly, then there is a sudden phase increase at 980 MeV indicating the presence of the $f_0(980)$. The modulus of the amplitude shows a dip at the mass of the

$f_0(980)$: intensity is taken from $\pi\pi$ scattering to the $K\bar{K}$ inelastic channel. The peak in the scattering amplitude at low energy is often called σ-meson; the second bump at 1300 MeV was called $\epsilon(1300)$. There is an on-going discussion on whether the σ should be considered as genuine meson or not; the interested reader may consult [60].

There are two processes which may contribute to the $\pi\pi$ scattering amplitude: formation of s-channel resonances and scattering via t-channel exchanges. They are schematically drawn in Fig. 18. Scattering processes or more precisely the scattering matrix can be expressed by a sum of s-channel resonances or t-channel exchanges; in Regge theory this is called duality and is the basis for the Veneziano model. So you may analyze a data set and describe the data by a sum over s-channel resonances and get a very good description with a finite number of complex poles in the $\pi\pi$ S-wave scattering amplitude. You could also analyze the data by a summation over t-channel exchange amplitudes and also get a good fit. If you add amplitudes for both processes, you run the risk of double counting. So in fits you should avoid to mix the two schemes.

There is a common believe that the interpretation of a pole in the complex scattering energy plane as originating from s-, t- or u-channel phenomenon is a matter of convenience. I do not share this view: only s-channel resonances have defined couplings to different final states, t- or u-channel exchanges have not. The q^2 dependence of t- or u-channel exchange processes reflects interaction ranges, the q^2 dependence of s-channel resonances reflects the spread of the wave function. When 'counting' the number of $q\bar{q}$ states (to argue that we have a decuplet of scalar states instead of a nonet), we have to count the number of 'true' s-channel resonances and have to suppress poles in the scattering plane which originate from t-channel exchange processes. The $f_0(400-1200)$, e.g., is certainly present in scattering data with a pole in the complex energy plane. And you may choose to describe this pole as s-channel resonance even if its true origin might be t-channel exchange.

We are searching for resonances in the s-channel, for poles originating from s-channel resonances. But there may also be poles due to t-channel exchanges, poles originating from meson-meson interactions. They should rather be interpreted as mesic molecules and not as $q\bar{q}$ mesons. So, how does one decide if a particular pole in the scattering plane is due to a s-channel resonance or to t-channel exchanges ?

s-channel resonances have always the same ratio of couplings to different final states. The partial widths of the $f_0(1500)$ must not depend on the way how it was produced. This is different for t-channel exchanges: assume the

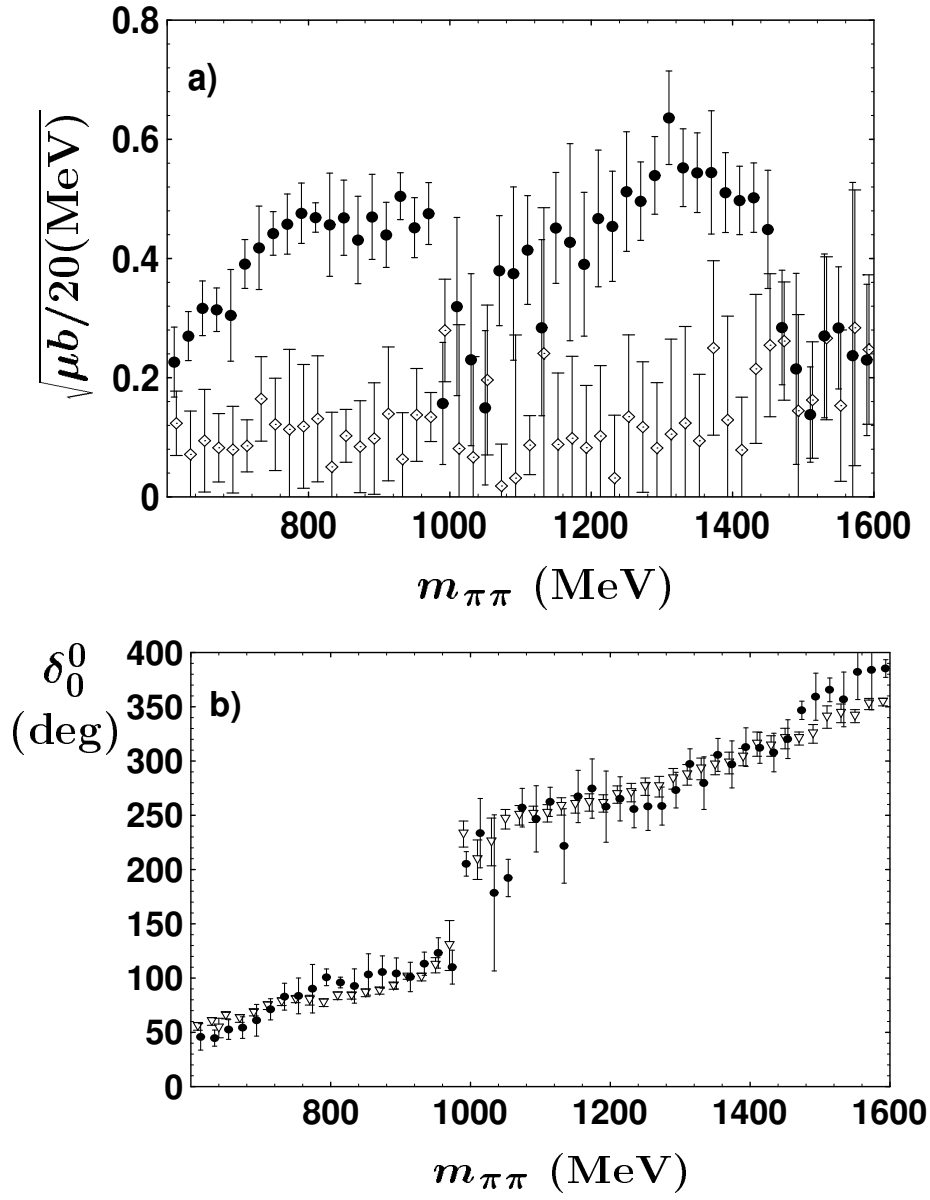

Figure 17: Amplitude and phase from $\pi\pi$ scattering (black dots); open circles: $\pi a_1(1260)$ scattering. Shown is the so-called down-flat solution; (from [61]).

$f_0(980)$ would be produced by t-channel exchanges only, then it could show up differently in $\pi\pi$ and in $K\bar{K}$ scattering. Properties of a 'resonance' which depend strongly on the production process suggest that the resonance may originate from t-channel exchanges.

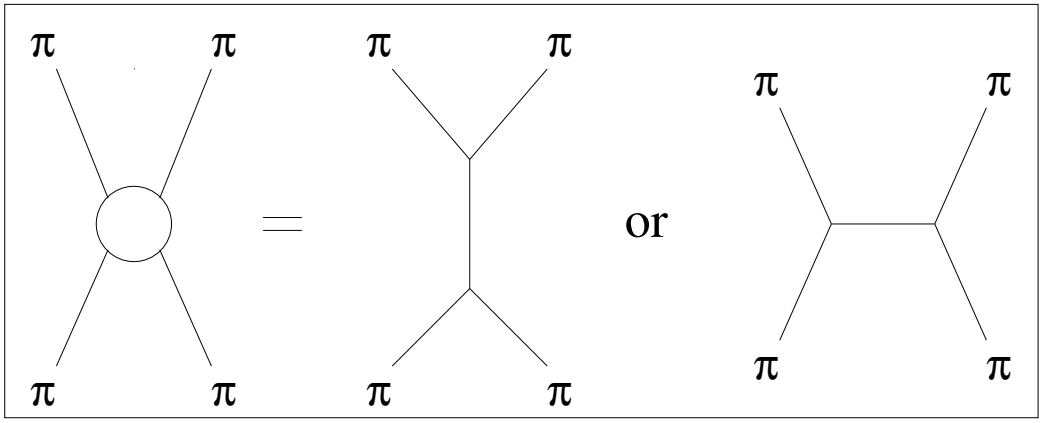

Figure 18: Scattering of two pions (left) via s-channel resonances (center) and t-channel exchange.

4.3.2 The *red dragon* in $\pi\pi$

The $\pi\pi$ scattering amplitude exhibits a continuously and slowly rising phase and a sudden phase increase at 980 MeV. The rapid phase motion is easily identified with the $f_0(980)$, the slowly rising phase can be associated with an s-channel resonance which was called $f_0(1000)$ by Morgan and Pennington [82]. It extends at least up to 1400 MeV. Minkowski and Ochs [66] suggested that this broad enhancement which they call *the red dragon* is the scalar glueball. However, we have seen that this broad background amplitude - including the monotonously rising phase - can well be reproduced by a ρ exchange amplitude in the t-channel. From a fit to the $\pi\pi$ S-wave scattering data even mass and width of the ρ exchanged in the t-channel can be determined. So this background amplitude is likely not a $f_0(1000)$ $q\bar{q}$ state, it is likely not two mesons, the old $\sigma(550)$ and $\epsilon(1300)$, it is caused by ρ (and possibly other less important) exchanges in the t-channel.

Fig. 19) shows data of the GAMS collaboration on $\pi\pi$ scattering from the charge exchange reaction π^- p$\rightarrow 2\pi^0$n at 40 GeV/c. At small momentum transfer, the $f_0(980)$ is produced as a dip. But at large momentum transfer, the dip disappears and the $f_0(980)$ shows up as a peak. I interprete this behavior as evidence that 'soft' processes like t-channel exchange dominate the scattering amplitude at small momentum transfer. At large momentum transfers the $q\bar{q}$ nature of the $f_0(980)$ core become the main feature of the data. The 'background' amplitude disappears at large t: the background is due to soft processes expanded over a larger volume. It is certainly not a compact and well localized glueball with properties as predicted in lattice gauge calculations.

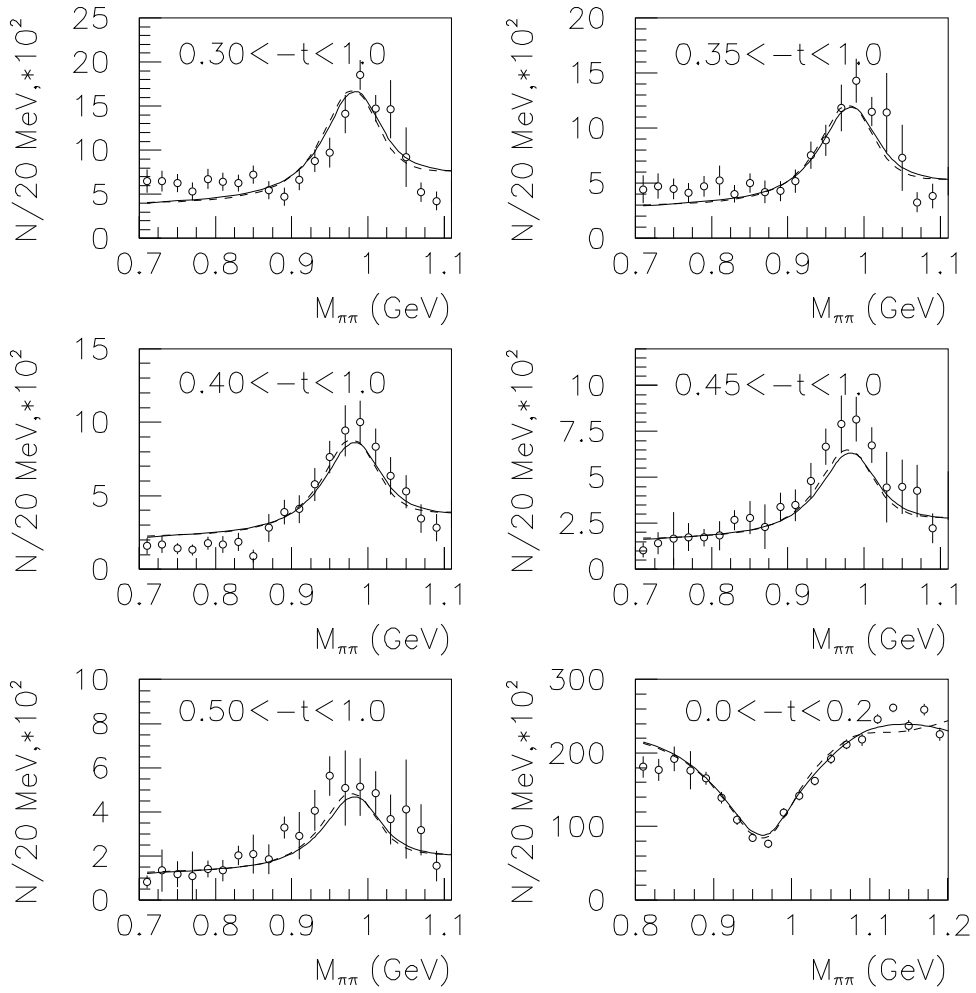

Figure 19: The $\pi\pi$ invariant mass distribution for different cuts in the momentum transfer t $= -q^2$ in the reaction π^-p$\to\pi^0\pi^0$n. At small t the $f_0(980)$ is observed as dip, for large momentum transfer as peak. The data are from [84], the fit from [85].

4.3.3 The *red dragon* in 4π

A similar question arises in the 4π final state. Is the enhancement seen in the left parts of Fig. 16 a $q\bar{q}$ resonance ? Or can it be traced to ρ and other exchanges in the t-channel ? We now argue that the latter is indeed the case.

First, consider Fig. 20. On the right side, a selection is made for small momentum transfers to the 4π system. At small momentum transfer, the

$f_0(1500)$ is seen as a dip. This resembles very much the data of the GAMS collaboration on $\pi\pi$ scattering (Fig. 19). But it also reminds us of the $J/\psi \to \gamma\pi^+\pi^-$ data (see Fig. 14) where a dip is seen at 1500 MeV instead of a peak.

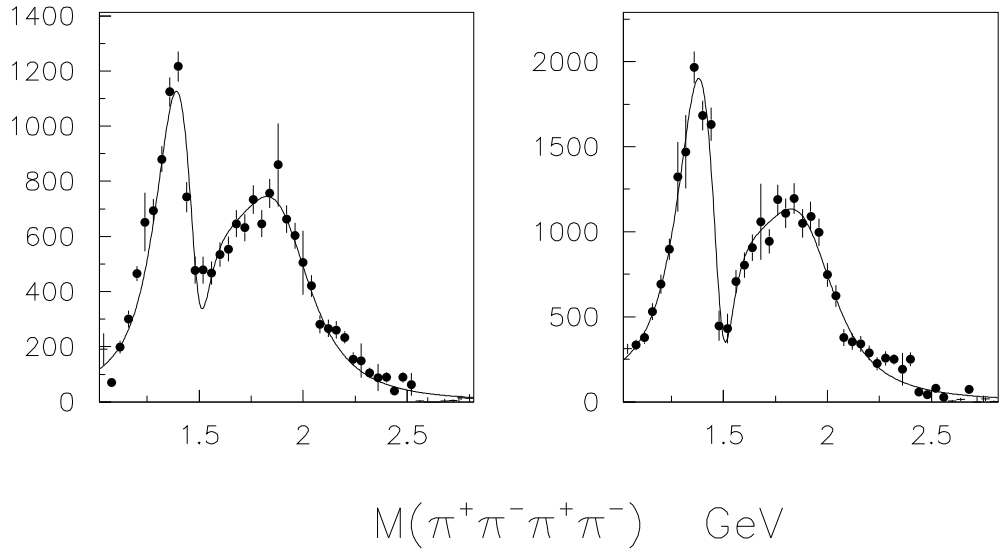

Figure 20: 4π invariant mass spectrum produced by two protons in central collisions. A cut is made on the angle in transverse direction between the two outgoing protons. Left: 90-135°, Right: 135-180°. The latter setting corresponds to the so-called glueball filter. The $f_0(1500)$ shows up as a dip just like the $f_0(980)$ in $\pi\pi$ scattering. From [81]

Consequently, we now make the attempt to interprete the 4π mass spectra of the WA102 experiment as t-channel exchange phenomenon in order to investigate if we gain further insight. We assume that Pomeron-Pomeron scattering can also proceed via ρ exchange in the t-channel. This t-channel amplitude then interferes with the production of the $q\bar{q}$ state $f_0(1500)$ producing a dip, very much alike the dip seen at 980 MeV in $\pi\pi$ scattering. Isospin conservation does not allow $\sigma\sigma$ production from ρ exchange in the t-channel for Pomeron-Pomeron scattering. We predict that at large momentum transfer the $f_0(1500)$ will also show up as peak.

Here we have made a first important step: we now understand why the left-hand spectra of Fig. 16 differ so much from the right-hand spectra. The $\sigma\sigma$ final state can be reached only via s-channel resonances and there is only one: the $f_0(1500)$. The $\rho\rho$ final state is produced by t-channel exchanges;

they generate the broad enhancement extending over the full accessible mass range. It rises at threshold for 4π production and falls off because of the kinematics of central production: high mass systems are suppressed with $1/\mathrm{M}^2$.

In contrast to Pomeron-Pomeron scattering, $\bar{\mathrm{p}}\mathrm{p}$ annihilation may also start from $\bar{\mathrm{p}}\mathrm{p}\to\rho\rho\pi$ which then converts via ρ exchange in the t-channel into $\sigma\sigma$. Hence we may expect $\rho\rho$ and $\sigma\sigma$ to contribute to the scalar isoscalar 4π mass spectrum.

We notice the similarity of the $f_0(1370)$ and the old $\epsilon(1300)$. The relation between these two phenomena is not well understood. The reason that the old $\epsilon(1300)$ was not identified with the $f_0(1370)$ lies just here: the $\epsilon(1300)$ was seen in $\pi\pi$ scattering with a small inelasticity, i.e. small coupling to 4π while the $f_0(1370)$ has small coupling to $\pi\pi$ and a large one to 4π. This is naturally explained when the 1300 MeV region interacts via t-channel exchange. Then $\pi\pi$ goes to $\pi\pi$, $\mathrm{K}\bar{\mathrm{K}}$ to $\mathrm{K}\bar{\mathrm{K}}$, Pomeron-Pomeron to $\pi\pi$ by pion exchange, to $\rho\rho$ via ρ exchange, etc.

There is one counter argument: the $\epsilon(1300)/f_0(1370)$ is not only a peak but it has also an intrinsic phase which varies by 180°. However, it is in the middle of two $q\bar{q}$ resonances. Two successive resonances in one partial wave have opposite phases. So there must be a phase advance of about 180°. This is not only the case for $\pi\pi$ scattering but must also be true for $\rho\rho$ scattering. $f_0(980)$ as scalar state must have a $\rho\rho$ coupling even though it cannot decay into $\rho\rho$ because of phase space limits. Hence the phase of the $\rho\rho$ scattering amplitude should raise from 980 to 1500 MeV by 180°. Due to the $\rho\rho$ threshold and the destructive interference with the $f_0(1500)$ the $\rho\rho$ scattering amplitude has a peak between 1000 and 1500 MeV: the most natural and economic description is by use of a Breit-Wigner resonance. But its true nature is of molecular character.

The interpretation suggested here can be tested: if the $f_0(1370)$ is a t-channel phenomenon it is produced with a phase of $\pm\pi/2$ with respect to the $f_0(980)$ and $f_0(1500)$.

We conclude that the $f_0(1370)$ is not produced in hard processes like J/ψ radiative decays, D_s decays or $\bar{\mathrm{p}}\mathrm{p}$ annihilation in flight, it is seen only in peripheral processes. The production and decay pattern in central production suggests that it is a t-channel phenomenon originating from meson-meson interactions.

4.3.4 Is the $\pi\pi$ low-mass enhancement the glueball?

In Pomeron-Pomeron scattering there is ample production of two-pions in S-wave. Data on $\pi^+\pi^-$ and $\pi^0\pi^0$ production for S-wave di-pions show a huge enhancement above the two-pion threshold. The $\pi\pi$ production in P-wave is strongly suppressed compared to $\pi\pi$ production in S-wave. This suppression supports the interpretation that central production is dominated by Pomeron-Pomeron scattering, that it is a gluon-rich process. Could this low-mass enhancement be the scalar glueball?

First we note that the question if the low-mass $\pi\pi$ interactions should be interpreted as s- or t-channel phenomenon cannot be decided by comparing different production and decay rates; below the opening of an inelastic channel the dependence of couplings to different final states cannot be investigated. On the other hand we know that the probability of Pomeron-Pomeron scattering scales with $1/M^2$ in the invariant mass. Taking this scaling into account, the data are fully compatible with the data from $\pi\pi$ scattering [86]. These data do not contain more glue than 'normal' $\pi\pi$ scattering data which can be understood quantitatively by ρ exchange amplitudes. The strong $\pi\pi$ production above threshold in central production does not evidence its glueball nature.

5 Interpretation

5.1 The spectrum of scalar mesons

After having argued that the $f_0(400-1200)$ and $f_0(1370)$, the red dragon of scalar isoscalar interactions, are likely generated by t-channel exchange amplitudes, we are left with 18 scalar states which can be grouped into 2 nonets. This is done in Table 7.

It must be emphasized again that the $f_0(980)$ and $f_0(1500)$ show a similar production and - partly also - decay pattern in $\pi\pi$ scattering and in D_s decays. In D_s decays it is appearant that the $f_0(980)$ and $f_0(1500)$ have no simple $u\bar{u}+d\bar{d}$ or $s\bar{s}$ structure: both are strongly produced in an $s\bar{s}$initial state and decay strongly to $\pi\pi$. This strong OZI rule violation is also observed in J/ψ decays into $\Phi\pi\pi$ and $\Phi K\bar{K}$.

The three states $f_0(1500)$, $f_0(1740)$ and $f_0(2100)$ have striking similarities in radiative J/ψ decays into 4 pions and $\bar{p}p$ annihilation in flight into

		$f_0(400-1200)^1$
	$a_0(980)^2$	$f_0(980)^2$
		$f_0(1370)^1$
$K_0^*(1430)^2$	$a_0(1490)^3$	$f_0(1500)^2$
		$f_0(1750)^3$
$K_0^*(1950)^3$		
		$f_0(2100)^3$

Table 7: The scalar mesons and their interpretation: [1]: generated by t-channel exchanges. [2]: The 1^3P_0 ground state scalar meson nonet. [3]: The 2^3P_0 first radially excited scalar meson nonet.

$\eta\eta$. These two reactions also show that the scalar isoscalar states are isolated non-overlapping resonances. The lowest state, the $f_0(980)$, is obviously strongly influenced by the K$\bar{\text{K}}$ threshold and its wave function must contain a large K$\bar{\text{K}}$ contribtion of molecular character. However, at large momentum transfer reactions, the $q\bar{q}$ nature of its core wave function becomes visible. The $f_0(980)$ should be produced in radiative J/ψ decays; it has however not been observed. This is certainly a hint which supports the interpretation of the $f_0(980)$ as K$\bar{\text{K}}$ molecule. On the other hand, also the $f_0(1500)$ is - at best - difficult to see in J/ψ decays. We have to wait for better data.

5.2 Instanton interactions

As we have discussed, the η and η' mesons are often considered as *gluish*. Let us discuss why this conviction is widely spread.

Most nonets have mixing angles which are close to the ideal one: there is a mainly $n\bar{n} = \sqrt{\frac{1}{2}}(u\bar{u} + d\bar{d})$ state and a $s\bar{s}$state. This is not true in the case of the pseudoscalar nonet: the η and η' mesons are not $n\bar{n}$ and $s\bar{s}$states but rather SU(3) octet and singlet states. You may try to understand this perturbatively. In vector mesons the $s\bar{s}$component needs at least 3 gluons to

convert into light quarks, in pseudoscalar mesons two gluons are sufficient. Hence the coupling between $n\bar{n}$ and $s\bar{s}$is much stronger for pseudoscalar (or scalar) mesons while it is weak for the other nonets. In other nonets like the tensor mesons you may invoke angular momentum barrier arguments to justify ideal mixing.

This picture has led to the conjecture that the η and η' wave functions should contain a glueball fraction. This conjecture is not supported experimentally. Also, the argument above does not consider the Goldstone nature of pseudoscalar mesons. In the limit of massless quarks, the pseudoscalar octet mesons should have vanishing masses, and the pseudoscalar mesons have indeed masses which are small compared to the nucleon mass. Only the η' has obviously not a small mass. Its mass originates from the coupling of the SU(3) singlet state to the gluon field. But this does not entail that there is a pure-glue component in the wave function in any point in space and time. The coupling between the η' and the gluon field can be described by introducing a new type of interactions based on instanton effects.

Quantization of the color fields leads to strong local fluctuations of the expectation values for $F^{\mu\nu}F_{\mu\nu}$ which can be localized as instanton solutions. The color fields generate a series of degenerate minima of the vacuum Hamiltonian (carrying different winding numbers) determining the propagation of massless quarks. Instantons and anti-instantons induce tunneling between the vacuum states. The tunneling to a state with a different winding number requires a flip of the helicities:

$$(S, M_s) \rightarrow (S, -M_s)$$

and are hence (in first order) restricted to interactions in pseudoscalar and scalar mesons since only here the total angular momentum J can remain unchanged when the spin is flipped. The strength of instantons changes sign for scalar mesons compared to pseudoscalar mesons but keeps its absolute value.

Instantons can be identified in lattice QCD and are found to have typical sizes of 0.36 fm. They are frequent: they are observed with a density (in space and time) of 1.6 $\mathrm{fm}^{-3} \cdot c\mathrm{fm}^{-1}$. Instantons induce spontaneous breaking of chiral symmetry leading to effective quark masses. They contribute to the vacuum condensate and provide an explanation for the axial anomaly.

Obviously, instantons mediate a very strong coupling between gluon fields and Goldstone bosons, in particular pions.

5.2.1 pseudoscalar mesons and Goldstone bosons

Let us now discuss the influence of instanton induced interactions on the pseudoscalar mass spectrum. Fig. 21 shows that instanton interactions bring the pion mass down and the η' mass up: the experimental masses of pseudoscalar mesons are very well reproduced. The calculated masses come from

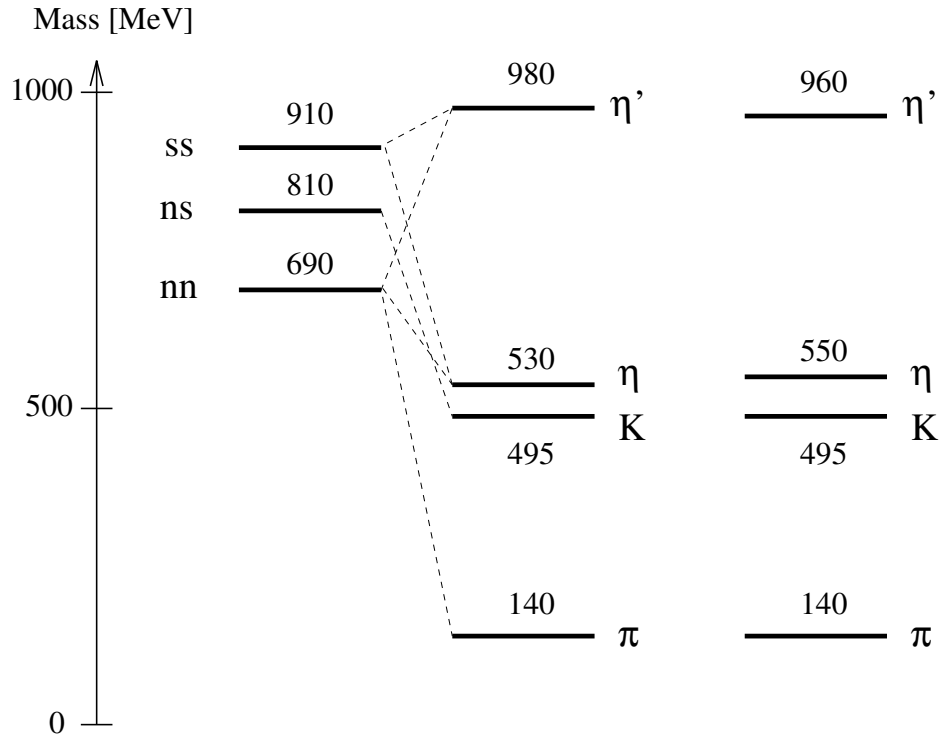

Figure 21: The mass spectrum of pseudoscalar mesons in a relativistic quark model using a linear confinement potential fitted to reproduce the Regge behavior and instanton interactions. Left: without, right including instanton interactions.

quark model calculations solving the Bethe Salpeter equation for a linear confinement potential the parameters of which are fitted to reproduce Regge trajectories [87]. There is no gluon exchange in the model; instead instanton interactions are used with a strength which is fitted to reproduce pseudoscalar meson mass spectrum. The confinement potential has a Lorentz structure which is chosen as $\frac{1}{2}(1 \otimes 1 - \gamma_0 \otimes \gamma_0)$. Alternatively, also a Lorentz structure given by $\frac{1}{2}(1 \otimes 1 - \gamma_\mu \otimes \gamma^\mu - \gamma_5 \otimes \gamma_5)$ was used.

5.2.2 Scalar mesons and instanton interactions

Fig. 22 shows the spectrum of scalar mesons as it is calculated now without using any new parameter [87]. The two predominantly isoscalar mesons are calculated to have masses of 980 and 1470 MeV, respectively. They are not $n\bar{n}$ and $s\bar{s}$states. The $f_0(980)$ is rather determined to be the SU(3) singlet state, nearly mass degenerated with the η'. The two isosinglet states η' and $f_0(980)$ form a parity doublet.

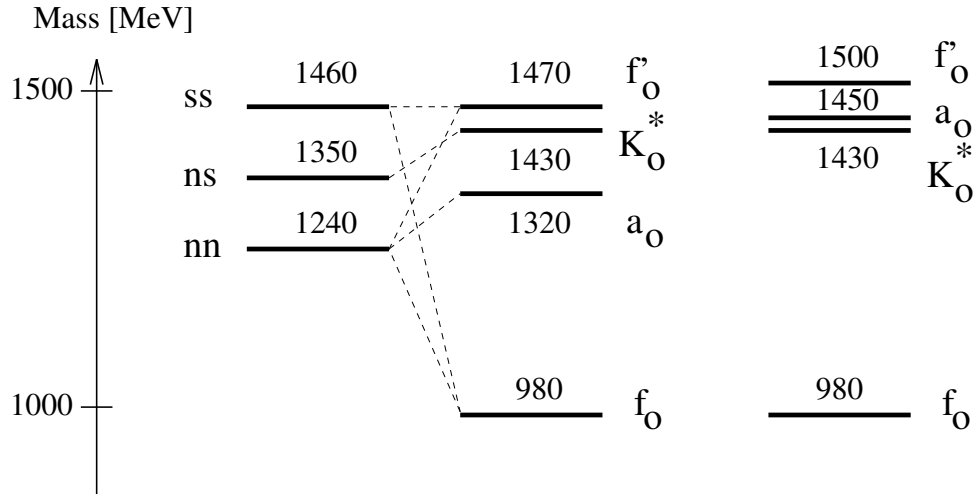

Figure 22: The mass spectrum of scalar mesons in a relativistic quark model using a linear confinement potential fitted to reproduce the Regge behavior and instanton interactions. Left: without, right including instanton interactions.

The full spectrum of scalar states calculated for the two different Lorentz structures of the confinement potential [89][88] are compared to experiment in Table 8. The octet state is found at 1470 MeV, it is readily identified with the $f_0(1500)$. From the T matrices for $\pi\pi\to\eta\eta$ and $K\bar{K}\to K\bar{K}$ scattering, Minkowski and Ochs [66] concluded that the $n\bar{n}$ and $s\bar{s}$ components of the $f_0(1500)$ must have opposite signs, an observation providing strong evidence against a large glueball component in the $f_0(1500)$ wave function.

The first radial excitations of the $f_0(980)$ and $f_0(1500)$ are calculated to have masses of 1776 and 2113 MeV, respectively. The agreement with the experimental candidates discussed above is excellent, much better than one could expect.

The calculated masses of the two isodoublets states K_0 also agree very well with the experimental values, but there is a problem in the isovector meson masses. The calculated values are 1320 and 1930 MeV, respectively. Experimentally, we have one state at 980 and one at 1480 MeV. The first one is suspected of being a $K\bar{K}$ molecule; the latter mass value is consistently found by the Crystal Barrel Collaboration in $\pi\eta$ [90] , $\pi\eta'$ [91] , and $K\bar{K}$ [92]. The Obelix Collaboration, however, finds a mass of 1290 MeV [93].

The agreement in the isovector sector is improved, the overall agreement weakened if a different Lorentz structure is chosen. Table 8 shows a comparison of the scalar mesons with calculated values using two different Lorentz structures for the confinement potential.

The results of model B are in striking agreement with the K matrix poles of a coupled-channel analysis of various reactions in which scalar states are produced [59]. (Note that the experimental entries in Table 8 correspond to poles in the scattering amplitude or T-matrix.) In this analysis, 5 poles are introduced. Four poles are enforced to make up two nonets with couplings which are fixed to guarantee SU(3) symmetry in their decays. The mixing angle of the nonets is a free parameter in the fit. One of the five poles is considered to be of exotic nature. Its decay modes are compatible with full flavor symmetry. In the scattering amplitude, this pole is rather wide: it has a mass in the range from $\sim$ 1200 to 1600 MeV and a width of about $\sim$ 1000MeV.

Their starting point is the observation that quark model calculations yield bare meson masses which could be and are effected by their couplings to decay channels. This coupling leads to particularly strong shifts in case of scalar mesons. The authors in [59] propose to identify the K-matrix poles with bare meson masses, T-matrix poles with the observed meson masses. This is an ansatz which is worth to be tested. The authors do not, however, discuss the nature of their 5 poles. From the discussion of $\pi\pi$ scattering, central production, radiative Jψ data, of $\bar{p}p \to \pi^0\eta\eta$ in flight and D_s decays I believe 3 scalar isoscalar resonances to exist below 1.8 GeV. Hence I believe that 2 of the poles in [59] are used to describe t-channel exchange processes. Of course, the presence of these poles has an impact on the position of all other poles. Therefore, in my view, this ansatz does not lead to a reliable and interpretable result. In spite of the striking agreement between the K-matrix analysis and model B, I am personally convinced that the results of the K-matrix analysis must be misleading.

Experiment			model A			model B		
	$a_0(980)$	$f_0(980)$		$a_0(1321)$	$f_0(984)$		$a_0(1057)$	$f_0(665)$
$K_0^*(1430)$	$a_0(1490)$	$f_0(1500)$	$K_0^*(1426)$	$a_0(1931)$	$f_0(1468)$	$K_0^*(1187)$	$a_0(1665)$	$f_0(1262)$
		$f_0(1740)$			$f_0(1776)$			$f_0(1554)$
$K_0^*(1950)$			$K_0^*(2058)$			$K_0^*(1788)$		
		$f_0(2100)$			$f_0(2113)$			$f_0(1870)$

Table 8: The scalar mesons in a relativistic quark model with an instanton-induced interaction. The two models are different in the Lorentz structure of the (linear) confinement potential. (A): $\frac{1}{2}(1 \otimes 1 - \gamma_0 \otimes \gamma_0)$; (B): $\frac{1}{2}(1 \otimes 1 - \gamma_\mu \otimes \gamma^\mu - \gamma_5 \otimes \gamma_5)$.

5.3 What is wrong with the scalar glueball ?

We have identified two full nonets of scalar mesons, no meson is left to play the role of the ground-state glueball. Also, the number of states is just what we expect from the quark model: there is no additional state, there is no evidence that the scalar glueball has intruded the spectrum of scalar quarkonia and mixes with them. Could the scalar glueball have escaped detection?

This is very unlikely. At least it is incompatible with experimental findings in radiative J/ψ decays. The 2π, K$\bar{\text{K}}$ and 4π intensities is measured, the full intensity is ascribed to conventional $q\bar{q}$ states. The scalar states are well separated; their mass difference is large compared to their widths. Their is no room for the scalar glueball to hide away. So the question arises how we can understand the absence of the scalar glueball which is so firmly predicted by QCD on the lattice.

The reason has to lay in the approximations made on the lattice. QCD on the lattice neglects the coupling of the gluon field to $q\bar{q}$ pairs, to pions, to Goldstone bosons. This is called quenched approximation. Recent glueball mass calculations on the lattice include couplings to fermion loops [109] but pions are still too heavy to represent the true chiral limit.

We may estimate the strength of this coupling from the pseudoscalar mixing angle. The η and η' mesons are nearly octet and singlet states, the $s\bar{s} - n\bar{n}$ mass difference leads to mixing with a mixing angle of about $-18°$

degrees or of 1/3 radian. In a basis of $n\bar{n}$ and $s\bar{s}$eigenstates the matrix element which mixes the two states is therefore large compared to the mass difference before mixing, large compared to $m_{s\bar{s}} - m_{n\bar{n}} \sim 300\,\mathrm{MeV}$. The matrix element for the transition $n\bar{n} \rightarrow$ gluon fields $\rightarrow s\bar{s}$ in the η or η' wave function must therefore be of the order of a GeV. Using the arguments advocated for by Schwinger [94] the transition $n\bar{n} \rightarrow$ gluon fields $\rightarrow s\bar{s}$ is a tunneling phenomenon through a potential barrier, with a probability which falls off exponentially with the generated quark mass. The energy gap to $s\bar{s}$is of course much larger than that to $n\bar{n}$: gluon fields must have a very large coupling to pions, and the scalar glueball may acquire a width of several GeV! Lattice gauge calculation do not have these small pion masses, they fail to observe the strong coupling of gluon fields to nearly massless quarks. The neglect of the Goldstone aspects of pseudoscalar mesons may lead to long-lived glueball states. If the coupling of gluon fields to light quarks is indeed governed by Schwinger's tunneling process, no resonant-like behavior of scalar gluon-gluon interactions are to be expected.

6 Hybrids

Hybrids, mesons with an intrinsic gluonic excitation, were first predicted shortly after the development of the bag model [13]. At that time, hybrids were thought of as $q\bar{q}$ pair in color octet neutralized in color by a constituent gluon [95, 96]. Today we expect hybrids as excitations of the gluon fields providing the binding forces between quark and antiquark, as excitations of the color flux tube linking quark and antiquark [97].

Hybrids are expected with a wide range of different quantum numbers. Particularly exciting is the possibility of states with exotic J^{PC} configurations like $J^{PC} = 1^{-+}$, with quantum numbers which are not accessible to $q\bar{q}$ systems [98]. They are expected at masses around 2 GeV and higher and to decay into two mesons with one of them having one unit of orbital angular momentum [99].

6.1 Exotica with $I^G(J^{PC}) = 1^-(1^{-+})$

6.1.1 The $\pi_1(1400)$

Indeed, an exotic meson has been seen to decay into a p-wave $\eta\pi$ system. The quantum numbers in this partial wave are $I^G(J^{PC}) = 1^-(1^{-+})$. These

are not quantum numbers which are accessible to the $q\bar{q}$ system, they are exotic.

A meson with quantum numbers $I^G(J^{PC}) = 1^-(0^{-+})$ is called a π, one with $I^G(J^{PC}) = 1^-(2^{-+})$ is called π_2. These latter two mesons are well established $q\bar{q}$ mesons. A meson with quantum numbers $I^G(J^{PC}) = 1^-(1^{-+})$ is thus called π_1. Its mass is added to the name in the form $\pi_1(1400)$ to identify the meson since there could be and there are more than one resonance in this partial wave.

A meson with exotic quantum numbers like the $\pi_1(1400)$ cannot be a regular $q\bar{q}$ meson. It must have a more complex structure. It could be a hybrid but it might also be a four-quark $qq\bar{q}\bar{q}$ resonance. The quantum numbers give no hint which of the two possibilities is realized in nature. Before we discuss arguments in favor of a four-quark assignment let us first have a look at the experimental findings.

At BNL, the reaction

$$\pi^- \; p \rightarrow \; \pi^- \eta \; p$$

was studied at 18 GeV/c [100][101]. The data show a large asymmetry in the angular distribution evidencing interference between even and odd angular momentum contributions. Fig. 23 shows data and the results of the partial wave analysis. In a scattering process, the $\pi\eta$ system can be produced in different partial waves (S, P, D waves). In the t-channel quantum numbers are exchanged corresponding to natural $(0^{++}, 1^{--}, 2^{++})$ or unnatural $(0^{-+}, 1^{+-}, 2^{-+})$ parity. The naturality is a good quantum number for a given partial wave and is added as suffix, + for natural, - for unnatural exchange.

The data are fully compatible with the existence of a resonance in the $I^G(J^{PC}) = 1^-(1^{-+})$ partial wave produced via natural parity exchange. Mass and width are fitted to values given in Table 9.

Since the spin in the final state is one, the exchanged particle cannot have scalar quantum numbers. The resonance is not observed in the charge exchange reaction [108] (with $\pi^0\eta$ in the final state), hence the exchanged particle cannot be the ρ. The particle which is exchanged is the $f_2(1270)$ (or the tensor part of a Pomeron).

The Crystal Barrel Collaboration studied the reaction $\bar{p}n \rightarrow \pi^-\pi^0\eta$. Fig. 24 shows the $\pi^-\pi^0\eta$ Dalitz plot. Clearly visible are $\rho^-\eta$, $a_2(1320)\pi$ with $a_2(1320) \rightarrow \eta\pi$ (in two charge modes) as intermediate states.

A fit with only conventional mesons gives a bad description only: the difference between data and predicted Dalitz plot shows a pattern which

is very similar to the contributions expected from the interference of the $\pi_1(1400)$ with the amplitudes for production of conventional mesons [102].

Introducing the exotic partial wave, the fit optimizes for values listed in Table 9. Selection rules (and the PWA) attribute the production of the exotic partial wave to the $\bar{\mathrm{p}}\mathrm{p}\ ^3S_1$ initial state.

A similar analysis on the reaction $\bar{\mathrm{p}}\mathrm{p}\to 2\pi^0\eta$ was carried out. In this case the $\pi_1(1400)$ can only be produced from the $^1S_0$ state; its production is much reduced in this situation. The small contribution could only be unrevealed when data taken by stopping antiprotons in liquid and gaseous H_2 where analyzed. In these two data sets the fraction of annihilation contributions from atomic S and P states is different (and their ratio known from cascade models). Thus S and P wave contributions are constrained. It is only under these conditions that positive evidence for the small contribution from the exotic partial wave could be found [103].

Experiment	mass (MeV/c^2)	width (MeV/c^2)	decay mode	reaction
BNL [100]	$1370 \pm 16\ ^{+\ 50}_{-\ 30}$	$385 \pm 40\ ^{+\ 65}_{-105}$	$\eta\pi$	$\pi^-\mathrm{p} \to \eta\pi^-\mathrm{p}$
BNL [101]	$1359\ ^{+\ 16}_{-\ 14}\ ^{+\ 10}_{-\ 24}$	$314\ ^{+31}_{-29}\ ^{+\ 9}_{-66}$	$\eta\pi$	$\pi^-\mathrm{p} \to \eta\pi^-\mathrm{p}$
CBar [102]	$1400 \pm 20 \pm 20$	$310 \pm 50\ ^{+50}_{-30}$	$\eta\pi$	$\bar{\mathrm{p}}\mathrm{n} \to \pi^-\pi^0\eta$
CBar [103]	1360 ± 25	220 ± 90	$\eta\pi$	$\bar{\mathrm{p}}\mathrm{p} \to \pi^0\pi^0\eta$
BNL [104]	$1593 \pm 8\ ^{+29}_{-47}$	$168 \pm 20\ ^{+150}_{-\ 12}$	$\rho\pi$	$\pi^-\mathrm{p} \to \pi^+\pi^-\pi^-\mathrm{p}$
BNL [105]	1596 ± 8	387 ± 23	$\eta'\pi$	$\pi^-\mathrm{p} \to \pi^-\eta'\mathrm{p}$
VES [106]	1610 ± 20	290 ± 30	$\rho\pi, \eta'\pi$	$\pi^-\mathrm{N} \to \pi^-\eta'\mathrm{N}$

Table 9: Evidence for $\mathrm{J^{PC}} = 1^{-+}$ exotics

6.1.2 The $\pi_1(1600)$

The $\pi_1(1400)$ is not the only resonance observed in this partial wave. At Serpukhov, the $\pi\eta'$, $\rho\pi$ and the $b_1(1235)\pi$ systems are studied in a 40 GeV/c π^- beam. In all three systems a resonant contribution in the exotic $I^G(J^{PC}) = 1^-(1^{-+})$ partial wave is found. A combined fit finds a mass of $\sim$1600 MeV and a width of $\sim$300 MeV [106]. Likely, these are three different decay modes of one resonances. Fig. 25 shows the VES data with fit.

At BNL, the $\eta'\pi$ is also observed to exhibit a resonant behaviour [105] at about 1600 MeV. A partial wave analysis of the $\rho\pi$ system [104] reveals an exotic meson with mass and width given in Table 9

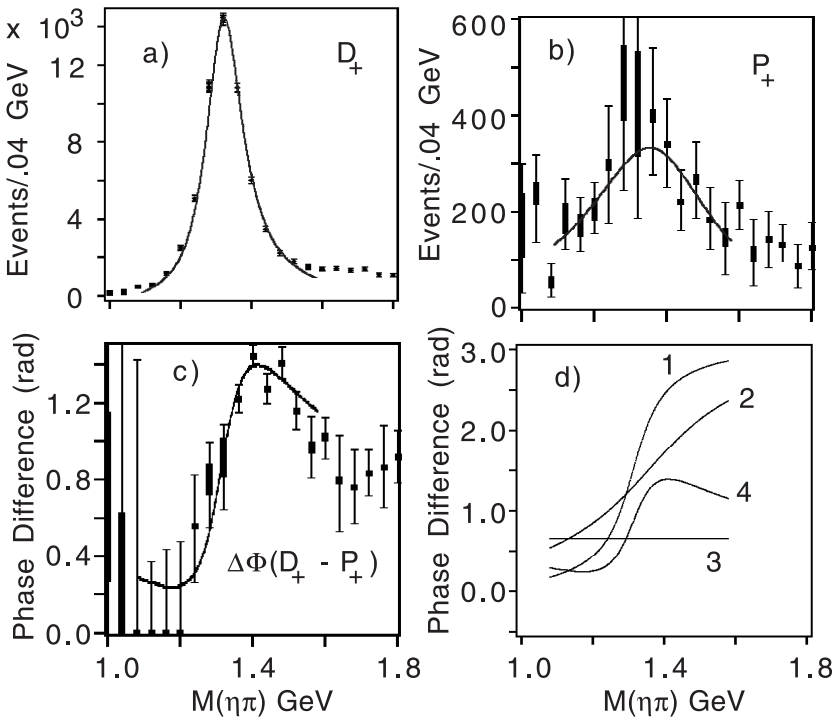

Figure 23: The squared scattering amplitude for the D^+ (a) and P^+ (b) waves. The +sign indicates natural parity exchange. amplitude. The relative phase between the two waves is shown in (c). The lines correspond to the expectation for two Breit-Wigner amplitudes. In (d) the (fitted) phases for the D- (1) and P-wave (2) are shown. The P- and D-production phases are free parameters in the fits; their differences are plotted as line 3 and - with a different scale - as 4.

6.1.3 Higher-mass exotics

There is evidence for further states from an analysis of $\pi^0 f_1(1285)$ production [107]. The two mesons are produced in part with zero orbital angular momentum between them, and this leads to the same quantum numbers we have seen so often now, to the exotic $I^G(J^{PC}) = 1^-(1^{-+})$ partial wave. The phase motion in this partial wave is not so well determined as in the other cases. It suggests that even two resonances might exist, at 1800 and 2100 MeV.

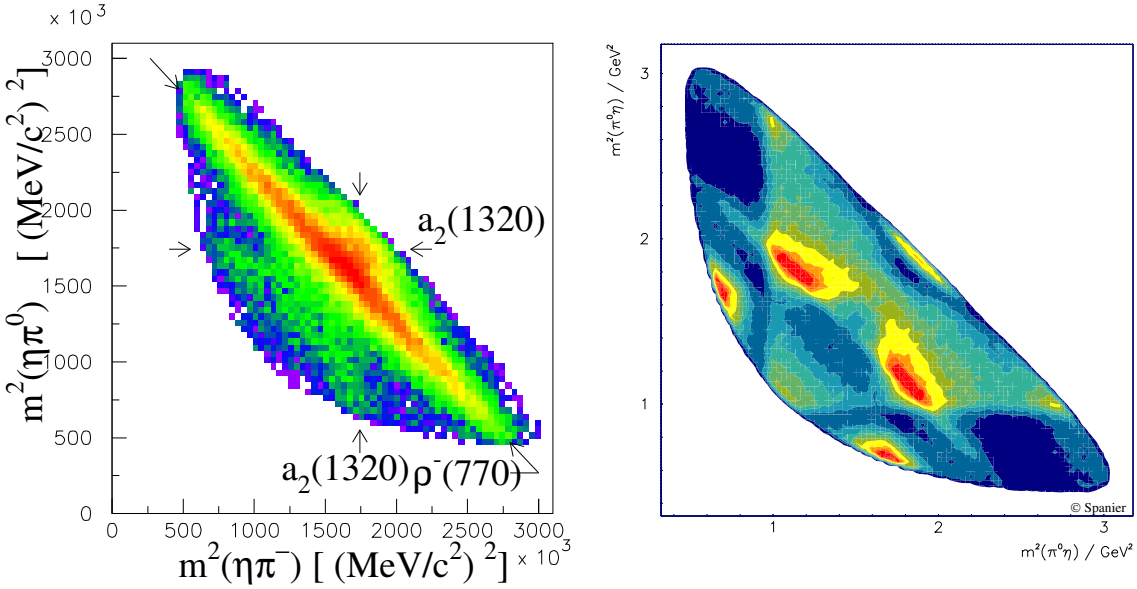

Figure 24: Dalitz plot for the reaction $\bar{p}n \to \pi^-\pi^0\eta$ for antiproton annihilation at rest in liquid D_2. Annhilation on quasi-free neutrons is enforced by a cut in the proton momentum ($p_{proton} \leq 100\,\mathrm{MeV/c}$. The data require contributions from the $I^G(J^{PC}) = 1^-(1^{-+})$ partial wave in the $\eta\pi$ system.

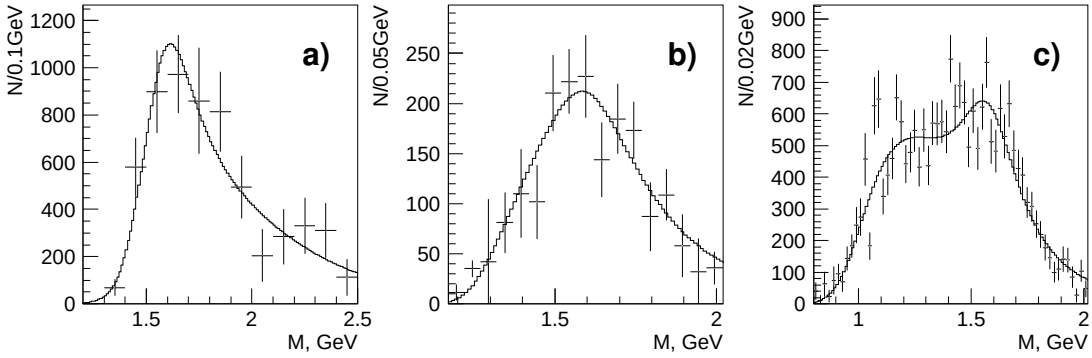

Figure 25: Intensities in the $I^G(J^{PC}) = 1^-(1^{-+})$ partial wave for the (from left to right) $b_1\pi$, $\eta\pi$ and $\rho\pi$ systems. The curves represent a fit to the data.

6.2 Four-quark or hybrid ?

Neither the $\pi_1(1400)$ nor the $\pi_1(1600)$ have a mass as predicted for hybrids; the $\pi_1(1400)$ does not have the predicted decay mode into a meson with one unit of orbital angular momentum. Only the $\pi_1(1600)$ decays into $b_1(1235)\pi$

but this decay mode is not particularly dominant. The exotic partial wave in the $\pi^0 f_1(1285)$ system at about 1800 MeV corresponds much more to what we should expect. Then the questions remains why so many resonances exist in this one partial wave. The large number of states in one partial and in such a narrow mass interval is certainly surprising. All have exotic quantum numbers, so they cannot possibly be $q\bar{q}$ states.

We now discuss whether they are likely four-quark states or the searched-for hybrid mesons.

6.2.1 The Fock-space expansion

The majority of established mesons can be interpreted as $q\bar{q}$ bound states. This can be an approximation only; the ρ-meson e.g. with its large coupling to $\pi\pi$ must have a four-quark component and could as well have contributions from gluonic excitations. The Fock space of the ρ must be more complicated than just $q\bar{q}$. We may write

$$\rho \ = \alpha q\bar{q} + \beta_1 b\bar{q}q\bar{q} + ... + \gamma_1 q\bar{q}g + ... \tag{8}$$

where we have used $q\bar{q}g$ as short-name for a gluonic excitation. The orthogonal states may be shifted into the $\pi\pi$ continuum. Now we may ask: are the higher-order terms important and what is the relative importance of the β and γ series ?

Possibly this question can be answered by truncating the α-term. Exotic mesons do not contain a $q\bar{q}$ component and they are rare. Naively we may expect the production of exotics in hadronic reactions to be suppressed by a factor 10 when one of the coefficients, α_1 or β_1, is of the order 0.3. We thus expect additional states having exotic quantum numbers, quantum numbers which are not accessible to the $q\bar{q}$ system. Their production rate should be suppressed compared to those for regular $q\bar{q}$ mesons. In non-exotic waves the four-quark and hybrid configurations are likely subsumed into the Fock expansion. If we can decide what kind of exotic mesons we observe, four-quarks or hybrids or both, we can say what the most important contributions in (8) are.

6.2.2 SU(3) relations

The $\pi_1(1400)$ decays strongly into $\pi\eta$, the $\pi_1(1600)$ into $\pi\eta'$; decays of the $\pi_1(1400)$ into $\pi\eta'$ and of the $\pi_1(1600)$ into $\pi\eta$ were not observed or reported.

Fig. 26 shows the exotic wave for the $\pi\eta$ and $\pi\eta'$ systems as a function of their mass: the $\pi\eta$ intensity is concentrated around 1400 MeV, the $\pi\eta'$ intensity at 1600 MeV. A resonance decaying into $\pi\eta'$ should also decay into $\pi\eta$, and a $\pi\eta$ resonance should also have a sizable coupling to $\pi\eta'$. Why is there such a strange decay pattern ?

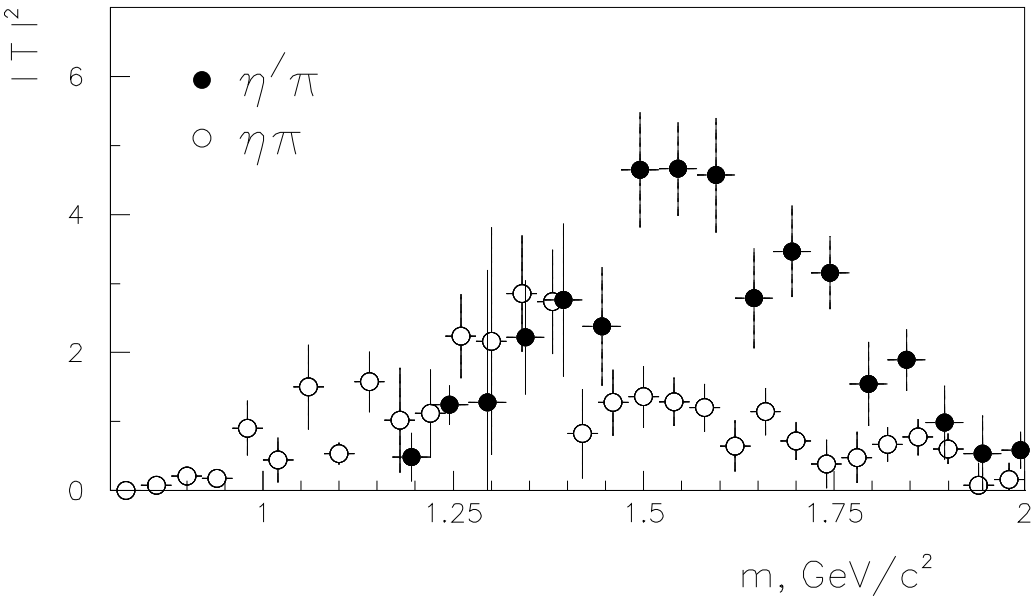

Figure 26: The squared scattering amplitude in the $I^G(J^{PC}) = 1^-(1^{-+})$ partial wave for the $\eta\pi$ and $\eta'\pi$ systems; (from [106]).

We first consider the limit of flavor symmetry: the η is supposed to belong to the pseudoscalar octet, the η' is considered as pure singlet SU(3) state; mixing is neglected. The π_1 states, having isospin one, cannot be isoscalar states. Now I claim, that a meson belonging to an octet with exotic quantum numbers $J^{PC} = 1^{-+}$ cannot decay into two octet pseudoscalar mesons.

The argument goes as follows: decays of particles belonging to an octet of states into two other octet mesons, decays of the type $8 \to 8 \otimes 8$ may have symmetric or antisymmetric couplings. The two octets can be combined using symmetric structure constants d_{ijk} or antisymmetric structure constants f_{ijk}. The decay $\pi_1(1400)$ into two pseudoscalar mesons is governed by the symmetric couplings. SU(3) demands the decay amplitude for decays into two pseudoscalar mesons not to change sign when the two mesons are exchanged. The orbital angular momentum $l = 1$ between the two mesons

requires the opposite: the two mesons must be in a state $\pi\eta$-$\eta\pi$. Both requirements cannot be fulfilled at the same time: the decay of a π_1 which belongs to an SU(3) octet into two octet pseudoscalar mesons is forbidden.

There are immediate consequences: let us begin with the $\pi_1(1600)$ and assume that it belongs to an octet of states. Then it must decay into $\pi\eta'$ while the decay into $\pi\eta$ is forbidden. This is precisely what we see. But what happens in case of the $\pi_1(1400)$? It does decay into $\pi\eta$, why ? As we have seen, it cannot belong to an SU(3) octet, hence it must belong to a multiplet of higher order. The easiest choice is a decuplet. The $\pi_1(1400)$ must be a SU(3) decuplet state ! As member of a decuplet, it cannot decay into $\pi\eta'$, into an octet and a singlet meson, and it cannot possibly be a hybrid: gluonic excitations do not contribute to the flavor. Mesonic hybrids can only be SU(3) singlets or octets. The strange phenomenon that the $\pi_1(1600)$ does not decay into $\pi\eta$ thus provides the clue for the interpretation of the $\pi_1(1400)$ as decuplet state.

The above arguments hold in the limit of flavor symmetry. Due to $\eta - \eta'$ mixing, the exotic $\pi_1(1600)$ could decay into $\eta\pi$ via the small singlet component of the η. Also a small coupling of the $\pi_1(1400)$ to $\eta'\pi$ is possible.

6.2.3 Four-quark states in SU(3)

In the limit of SU(3) symmetry, the $\pi_1(1400)$ with its large $\pi\eta$ decay rate must belong to a decuplet and must hence be a four-quark state. The $\pi_1(1600)$ must belong to an octet of states and could thus be a hybrid. There is no rigid argument against this conjecture. However, the mass difference between the $\pi_1(1400)$ and $\pi_1(1600)$ is typical for SU(3) multiplet splittings. It has the same order of magnitude as the octet-decuplet splitting in baryon spectroscopy, only the mass ordering is reversed.

Now let us dicuss how we can construct a decuplet of states from two quarks and two antiquarks. Two quarks in flavor 3 combine to $3 \otimes 3 = \bar{3} + 6$, two antiquarks to $3 + \bar{6}$. Now we construct

$$(\bar{3} + 6) \otimes (3 + \bar{6}) = \bar{3} \otimes 3 + \bar{3} \otimes \bar{6} + 6 \otimes 3 + 6 \otimes \bar{6}$$

$$= 1 + 8 + 8 + 10 + 8 + \bar{10} + 1 + 8 + 27$$

Hence we can construct $10 + \bar{10}$ and $10 - \bar{10}$ multiplets and four different octets. Hence a large number of different states with the same quantum numbers should be expected from four-quark states.

6.2.4 Exotic(s) summary

Several exotic mesons are observed, all in one partial wave $I^G(J^{PC}) = 1^-(1^{-+})$. The decay pattern of the two resonances at 1400 and 1600 MeV suggests that the $\pi_1(1400)$ should be a four-quark resonance belonging to a decuplet of states. Then further resonances with quantum numbers $I^G(J^{PC}) = 1^-(1^{-+})$ are to be expected and may have been found.

Even though there is no argument against the hypothesis that one of the observed resonances could be a hybrid, there is also at present no experimental support for this hypothesis. Once Pandora's box of four-quark states being open, it is very hard to establish experimentally that mesons with gluonic excitations be found in an experiment.

7 Conclusions

This review challenges the wide-held believe that gluons may act as constituent parts of hadronic matter. Gluons exist as we know, e.g. from 3-jet events in e^+e^- annihilation. Gluons interact; this we know from the jet distribution in 4-jet events in e^+e^- annihilation. Gluons are confined since they carry color. Do these facts imply that glueballs must exist ? I do not believe so. Let us recall what a resonance is: it may be defined, of course, in many different ways but it needs to have specific decay modes, and a phase variation must be associated with it. If the gluon-gluon interactions lead to such a fast coupling to final state particles that the phase advance during its life time is, let's say 1 degree, you cannot identify a resonant phase motion and the statement 'a glueball exists' looses its meaning.

What is the experimental basis for this interpretation ?

First we discuss glueballs. Scalar isoscalar interactions play an important role in many reactions. In purely hadronic reactions its is difficult to decide if a resonance or better a pole in the complex energy plane originates from a true s-channel resonance or if it originates from t-channel exchange processes. I believe that both types of reactions can lead to observable poles and that one has to identify those which come from s-channel resonances. The dependence on the momentum transfer in the production discriminates long-range t-channel exchange processes from s-channel resonances. Also, s-channel resonances have defined couplings to its different decay modes while e.g. ρ exchange scatters $\pi\pi$ dominantly to $\pi\pi$, Pomeron-Pomeron to $\pi\pi$ or to $\rho\rho$, $K\bar{K}$ to $K\bar{K}$, and so on.

In the glueball-$q\bar{q}$-scalar-meson mixing scenarios no attempt was made to exclude poles originating from t-channel exchange processes. One of the poles is however - as discussed at length in this review - likely due to such processes. This observation reduces the number of s-channel resonances which has of course significant impact on the mixing scenarios. With the $f_0(980)$ included in the list of $q\bar{q}$ mesons, the $f_0(1500)$ and $f_0(1740)$ belong to different nonets, to the 1^3P_0 ground state nonet and to the first radial excitations.

The broad 'background' component in scalar isoscalar interactions depends on the momentum transfer in a way which shows that its physical origin is a long-range process. So it cannot be the compact ground-state scalar glueball expected from lattice QCD.

There are processes which are free (or at least less influenced) by t-channel exchanges. These are Z^0 or J/ψ decays, radiative J/ψ decays, D_s decays. Even in these processes t-channel exchange may contribute: the data on Fig. 14c on the left side seem to suggest that the two gluons in radiative J/ψ decays may interact via pion exchange to create a two-pion pair and that this process interferes with $f_0(1500)$ production, the characteristic feature being the dip at 1500 MeV in the $\pi\pi$ mass distribution.

Unfortunately, data from experiments with a cleaner environment are statistically poor or - in case of Z^0 decays - difficult to analyze. From BES we hope for a significant increase in statistics in radiative or non-radiative J/ψ decays, the Babar experiment will deliver high-statistics data on D_s decays into three pions. In this review large credibility is laid on these reactions with scarce statistics. This is certainly a weak point. So you should take the article as contribution to an ongoing discussion.

We now turn to the discussion of exotic mesons. First we have to make the point that at least two exotic mesons, mesons with quantum numbers $I^G(J^{PC}) = 1^-(1^{-+})$ which cannot be reached within the $q\bar{q}$ scheme, now have been seen in different experiments which come to (nearly) consistent results for masses and widths for these states. This is great progress! These mesons can be four-quark states or hybrids. Here I argue that the decay pattern of the $\pi_1(1400)$ and $\pi_1(1600)$ suggests that these two states should be four-quark states. In the case of the two π_1 states, a decision on their hybrid or four-quark nature can be based on selection rules. In other cases, in particular in those in which non-exotic quantum numbers, the decision has to be based on dynamical arguments. Obviously, it is then very hard to argue that resonances should be interpreted as hybrids and not as four-quark states. As the first exotic states observed experimentally can be interpreted as four-quark states, production of four-quark states seems to be more likely than production of hybrids – if the latter exist at all.

I would like to draw the following consequences for our understanding of low-energy QCD:

Fundamental predictions of lattice gauge theory are challenged by data and their interpretation offered here. It is possible that lattice gauge theories are still too far away from the chiral limit. The assumption that static potentials QCD potentials can be calculated by simulating QCD on a lattice seems to be unjustified. Lattice QCD does - at present - not work sufficiently close to the chiral limit, it does not reproduce the Goldstone nature of pions and thus leads to wrong predictions concerning the existence of new types of hadronic matter, of glueballs and hybrids. We have to revise our understanding of low-energy QCD.

Acknowledgments

I would like to thank the Organizers of the Zuoz Summer School for the invitation to this beautiful place and the opportunity to talk about glueballs, hybrids and $q\bar{q}$ mesons. I appreciate the help of many colleagues in numerous discussions and would like to express my gratitude to those who have given advice, comments and help when I prepared and wrote this review. They often do not share my view; whenever you disagree with interpretations offered here you should not held them responsible. A few of them need to be mentioned here: V.V. Anisovich, S.U. Chung, A. Kirk, V. Markushin, B. Metsch, P. Minkowski, W. Ochs, M. Pennington, H. Petry, U. Thoma and H. Willutzki.

References

[1] M. Gell-mann and Y. Ne'eman, *The eightfold way*, Benjamin, New York, 1964

[2] J. D. Bjorken and E. A. Paschos, Phys. Rev. **185** (1969) 1975.

[3] J. J. Aubert *et al.*, Phys. Rev. Lett. **33** (1974) 1404.

[4] J. E. Augustin *et al.*, Phys. Rev. Lett. **33** (1974) 1406.

[5] H. Fritzsch and P. Minkowski, Nuovo Cim. **A30** (1975) 393.

[6] H. P. Dürr, Phys. Rev. Lett. **34** (1975) 422.

[7] H. P. Dürr, Phys. Rev. Lett. **34** (1975) 616.

[8] S. Weinberg, Phys. Rev. Lett. **31** (1973) 494.

[9] H. Fritzsch, M. Gell-Mann, H. Leutwyler, Phys. Lett. **B47** (1973) 365.

[10] K. G. Wilson, Phys. Rev. **D10** (1974) 2445.

[11] S. Coleman and D. J. Gross, Phys. Rev. Lett. **31** (1973) 851.

[12] J. Goldstone, Nuovo Cim. **19** (1961) 154.

[13] A. Chodos *et al.*, Phys. Rev. **D10** (1974) 2599.

[14] N. Isgur and G. Karl, Phys. Rev. **D20** (1979) 1191.

[15] Y. Nambu and G. Jona-Lasinio, Phys. Rev. **122** (1961) 345.

[16] N. Isgur and J. Paton, Phys. Lett. **B124** (1983) 247.

[17] W. H. Blask *et al.*, Z. Phys. **A337** (1990) 327.

[18] M. A. Shifman, A. I. Vainshtein and V. I. Zakharov, Nucl. Phys. **B147** (1979) 385.

[19] G. S. Bali, K. Schilling and A. Wachter, Phys. Rev. **D56** (1997) 2566

[20] G. S. Bali, K. Schilling and A. Wachter, in *NONE* hep-ph/9611226.

[21] R. M. Baltrusaitis *et al.*, [MARK-III Collab.], Phys. Rev. **D32** (1985) 2883.

[22] D. Coffman *et al.*, [MARK-III Collab.], Phys. Rev. **D38** (1988) 2695.

[23] J. Jousset *et al.*, [DM2 Collab.], Phys. Rev. **D41** (1990) 1389.

[24] M. Benayoun, L. DelBuono and H. B. O'Connell, Eur. Phys. J. **C17** (2000) 593

[25] P. Gavillet, R. Armenteros, M. Aguilar-Benitez, M. Mazzucato and C. Dionisi, Z. Phys. **C16** (1982) 119.

[26] J. S. Suh [Crystal Barrel Collab.], *In *Frascati 1999, Hadron spectroscopy* 555-560.*

[27] M. Acciarri *et al.* [L3 Collab.], hep-ex/0011035.

[28] J. Adomeit *et al.* [Crystal Barrel Collab.], Z. Phys. **C71** (1996) 227.

[29] D. E. Groom *et al.*, Eur. Phys. J. **C15** (2000) 1.

[30] K. Peters and E. Klempt, Phys. Lett. **B352** (1995) 467.

[31] S. Godfrey and J. Napolitano, Rev. Mod. Phys. **71** (1999) 1411

[32] H. Fritzsch and P. Minkowski, Annals Phys. **93** (1975) 193.

[33] C. J. Morningstar and M. Peardon, Phys. Rev. **D60** (1999) 034509

[34] S. Narison, Nucl. Phys. **B509** (1998) 312.

[35] D. Robson, Nucl. Phys. **B130** (1977) 328.

[36] C. Amsler, Rev. Mod. Phys. **70** (1998) 1293 [hep-ex/9708025].

[37] C. J. Batty, Rept. Prog. Phys. **52** (1989) 1165

[38] A. Abele *et al.* [Crystal Barrel Collab.], Eur. Phys. J. **C17** (2000) 583

[39] C. Amsler *et al.*, Phys. Lett. **B342** (1995) 433.

[40] C. Amsler *et al.* [Crystal Barrel Collab.], Phys. Lett. **B353** (1995) 571.

[41] C. Amsler *et al.* [Crystal Barrel Collab.], Phys. Lett. **B340** (1994) 259.

[42] A. Abele *et al.* [Crystal Barrel Collab.], Phys. Lett. **B385** (1996) 425.

[43] C. Amsler *et al.* [Crystal Barrel Collab.], Phys. Lett. **B322** (1994) 431.

[44] A. Abele *et al.* [Crystal Barrel Collab.], Phys. Lett. **B380** (1996) 453.

[45] The Crystal Barrel Collab., *Study of f_0-decays into four neutral pions*, submitted to Eur. Phys. J. C

[46] The Crystal Barrel Collab., *4π-decays of scalar and vector mesons* submitted to Eur. Phys. J. C

[47] J. Weinstein and N. Isgur, Phys. Rev. D27 (1983) 588

[48] R. Jaffe, Phys. Rev. **D15** (1977) 267,281.

[49] B.S. Zou, D.V. Bugg, Phys.Rev.D50 (1994) 591

[50] M.P. Locher, V.E. Markushin, H.Q. Zheng E.P.J. C4 (1998) 317

[51] G. Janssen *et al.*, Phys.Rev. **D52** (1995) 2690

[52] N. A. Tornqvist, Z.Phys. C68 (1995) 647

[53] C. Amsler and F.E. Close, Phys. Lett. **B353** (1995) 385; Phys. Rev. **D53** (1996) 295.

[54] W. Lee and D. Weingarten, Phys. Rev. **D61** (2000) 014015

[55] D. Li, H. Yu and Q. Shen, "Glueball-quarkonia content of the f0(1370), f0(1500) and f0(1710)," hep-ph/0001107.

[56] F. E. Close and A. Kirk, Phys. Lett. **B483** (2000) 345.

[57] L. S. Celenza *et al.*, Phys. Rev. **C61** (2000) 035201.

[58] M. Strohmeier-Presicek *et al.*, Phys. Rev. **D60** (1999) 054010

[59] A. V. Anisovich *et al.*, Z. Phys. **A357** (1997) 123.
A. V. Anisovich, V. V. Anisovich and A. V. Sarantsev, Phys. Lett. **B395** (1997) 123

[60] M. R. Pennington, "Riddle of the scalars: Where is the sigma?," *Workshop on Hadron Spectroscopy (WHS 99), Rome, Italy, March 1999.* hep-ph/9905241.

[61] R. Kaminski, L. Lesniak and K. Rybicki, Z. Phys. **C74** (1997) 79

[62] N. N. Achasov, S. A. Devyanin, G. N. Shestakov, Phys. Lett. **B96** (1980) 168.

[63] A. Bohrer, Phys. Rept. **291** (1997) 107.

[64] K. Ackerstaff *et al.*,Eur. Phys. J. **C4** (1998) 19.

[65] M. Boglione and M. R. Pennington, Eur. Phys. J. **C9** (1999) 11

[66] P. Minkowski and W. Ochs, Eur. Phys. J. **C9** (1999) 283.

[67] M. N. Achasov *et al.*, Phys. Lett. **B485** (2000) 349.

[68] F. E. Close, N. Isgur and S. Kumano, Nucl. Phys. **B389** (1993) 513.

[69] V. E. Markushin, Eur. Phys. J. **A8** (2000) 389

[70] E. Marco, S. Hirenzaki, E. Oset, H. Toki, Phys. Lett. **B470** (1999) 20

[71] M. N. Achasov *et al.*, Phys. Lett. **B479** (2000) 53

[72] O. Krehl, R. Rapp and J. Speth, Phys. Lett. **B390** (1997) 23

[73] F. E. Close and A. Kirk, Phys. Lett. **B489**, 24 (2000)

[74] M. Boglione and M. R. Pennington, Phys. Rev. Lett. **79** (1997) 1998

[75] R. Barate *et al.* [ALEPH Collab.], Phys. Lett. **B472** (2000) 189

[76] Dunwoodie, W., 1997, SLAC-PUB-7163, and *Proceedings of the Seventh International Conference on Hadron Spectroscopy* Brookhaven National Laboratory, Aug. 1997, American Institute of Physics, Conference Proceedings n.432.

[77] J. Z. Bai *et al.*, Phys. Lett. **B472** (2000) 207.

[78] D. V. Bugg, I. Scott, B. S. Zou, V. V. Anisovich, A. V. Sarantsev, T. H. Burnett and S. Sutlief, Phys. Lett. **B353** (1995) 378.

[79] T. A. Armstrong *et al.*, Phys. Lett. **B307** (1993) 394.

[80] D. Barberis *et al.*,Phys. Lett. **B471** (2000) 440

[81] D. Barberis *et al.* Phys. Lett. **B474** (2000) 423

[82] D. Morgan and M. Pennington, Phys. Rev. **D48** (1993) 1185.

[83] Liang-Ping Chen *et al.* [MARK III Collab.], SLAC-PUB-5669

[84] D. Alde *et al.* [GAMS Collab.], Z. Phys. **C66** (1995) 375.

[85] V. V. Anisovich and A. V. Sarantsev, Phys. Lett. **B382** (1996) 429

[86] A. Kirk, private communication

[87] E. Klempt, B. C. Metsch, C. R. Munz and H. R. Petry, Phys. Lett. **B361** (1995) 160

[88] R. Ricken, M. Koll, D. Merten, B. C. Metsch and H. R. Petry, hep-ph/0008221.

[89] M. Koll, R. Ricken, D. Merten, B. C. Metsch and H. R. Petry, Eur. Phys. J. **A9**, 73 (2000)

[90] C. Amsler *et al.* [Crystal Barrel Collab.], Phys. Lett. **B333** (1994) 277.

[91] A. Abele *et al.* [Crystal Barrel Collab.], Phys. Lett. **B404** (1997) 179.

[92] A. Abele, Phys. Rev. **D57** (1998) 3860.

[93] A. Masoni, Eur. Phys. J. **C8** (1999) 385.

[94] J. Schwinger, Phys. Rev. **82** (1951) 664.

[95] D. Horn and J. Mandula, Phys. Rev. **D17** (1978) 898.

[96] T. Barnes, F. E. Close, F. de Viron and J. Weyers, Nucl. Phys. **B224** (1983) 241.

[97] N. Isgur and J. Paton, Phys. Rev. **D31** (1985) 2910.

[98] F. E. Close and P. R. Page, Nucl. Phys. **B443** (1995) 233

[99] N. Isgur, R. Kokoski and J. Paton, Phys. Rev. Lett. **54** (1985) 869.

[100] D. R. Thompson *et al.* [E852], Phys. Rev. Lett. **79**, (1997) 1630

[101] S. U. Chung *et al.* [E852 Collab.], Phys. Rev. **D60** (1999) 092001

[102] A. Abele *et al.* [Crystal Barrel Collab.], Phys. Lett. **B423** (1998) 175.

[103] A. Abele *et al.* [Crystal Barrel Collab.], Phys. Lett. **B446** (1999) 349.

[104] G. S. Adams *et al.* [E852 Collab.], Phys. Rev. Lett. **81** (1998) 5760.

[105] S. U. Chung, *In *Frascati 1999, Hadron spectroscopy* 603-607.*

[106] Y. Khokhlov [VES Collab.], Nucl. Phys. **A663**, 596 (2000).

[107] J. H. Lee *et al.*, Phys. Lett. **B323** (1994) 227.

[108] S.U. Chung, private communication

[109] G. S. Bali *et al.* [SESAM Collab.], Phys. Rev. **D62** (2000) 054503